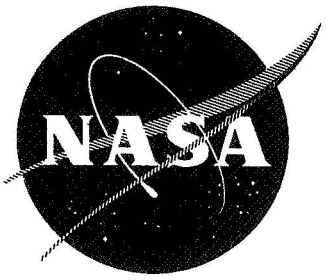

Progress Report No. 10

15 February 1969 to 15 May 1969

TOTAL ENERGY DISTRIBUTION MEASUREMENTS OF FIELD EMITTED ELECTRONS

By

L. W. Swanson
L. C. Crouser

Prepared for

Headquarters
National Aeronautics and Space Administration
Washington, D. C.

August 1969

CONTRACT NASw-1516

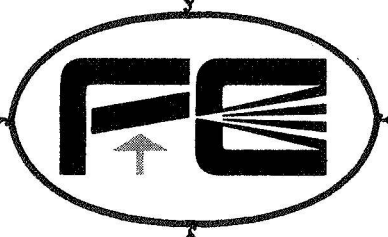

Field Emission Corporation

McMinnville, Oregon

Requests for copies of this report should be referred to

National Aeronautics and Space Administration
Office of Scientific and Technical Information
Attention: AFSS-A
Washington, D.C. 20546

Progress Report No. 10

15 February 1969 to 15 May 1969

TOTAL ENERGY DISTRIBUTION MEASUREMENTS OF FIELD EMITTED ELECTRONS

By

L. W. Swanson
L. C. Crouser

Prepared for

Headquarters
National Aeronautics and Space Administration
Washington, D. C.

August 1969

CONTRACT NASw-1516

PREFACE

This report describes work being performed under support from NASA, Headquarters, Washington, D. C. under contract NASw-1516. Our primary objective during this period is to explore the total energy distribution (TED) measurements of field emitted electrons in regards to the effect of adsorption. In particular we wish to understand the cause of the structure observed on the TED when polyatomic molecules are adsorbed at the surface.

INTRODUCTION

Experimental studies by Lambe and Jaklevic[1] of MOM tunneling junctions and Thompson[2] of Schottky barrier MS diodes have shown that tunneling electrons are inelastically scattered by polyatomic molecules adsorbed in the diode interface. This particular electron-phonon interaction mechanism was revealed experimentally by an enhancement in the diode conductance at various diode bias voltages characteristic of the vibronic spectra of the adsorbed molecule. Thus, a novel molecular spectrometer covering a wide range of wavelengths from the microwave to the visible and possessing a resolution of the order of 5 kT was unveiled by these findings.

Another mechanism by which adsorbates perturb the tunneling electrons is through a transmission resonance caused by wave mechanical interference effects due to the presence of discrete atomic potentials lying outside the main electronic charge cloud of the bulk metal. This mechanism was analyzed mathematically by Duke and Alferieff[3] who employed a one-dimensional pseudopotential model. According to their results atomic or molecular levels of an adsorbed particle lying within the conduction band provide windows of enhanced electron tunneling which can be most readily detected by analyzing the total energy distribution (TED) of the emitted electrons.

The prospect of detecting either or both of these effects on field emitted electrons at the metal-vacuum interface has prompted us to investigate the TED of vacuum field emitted electrons from substrates with chemisorbed monomolecular films. Useful information regarding the perturbation of the electronic and/or vibronic levels of the adsorbate by the adsorption act is potentially accessable from such measurements. In addition, the possibility of illucidating certain aspects of surface catalytic mechanisms in the chemisorption process portends to be a technologically useful derivative of these measurements.

Initial efforts in this direction using phthalocyanine (pht), primarily because of its large size and ease of handling in high vacuum, have been reported.[4]

In this report further results and interpretations of the phthalocyanine work are given along with preliminary results from pentacene adsorbed on the (310) plane of W. Evidence that both electronic and vibronic spectral information can be obtained by energy analysis of the field emitted electrons transmitted through large organic molecules is given.

THEORETICAL CONSIDERATIONS

A theoretical description of the effect of adsorbed molecules on the energy distribution of field emitted electrons with respect to tunnel resonance[3] and electron-phonon interaction[1] has been given. As pointed out in a previous report the large cross sectional area of these organic molecules should enhance detection of low transition probability phenomena.[4]

In addition to tunnel resonance and electron-phonon interaction, a third possibility to be considered is electron-electron interaction. Organic molecules such as those studied here possess low lying electronic states, e. g. , singlet and triplet, which can be excited by the tunneling electrons. In other words we have the possibility of elastic scattering of the tunneling electrons through tunnel resonance and/or inelastic scattering through two possible mechanisms, electron-phonon and electron-electron interactions.

It would be helpful to summarize the qualitative theoretically expected experimental manifestations of the above mentioned mechanisms. Basically there are four experimental observables which can be compared with experimental predictions; they are as follows:

1) the overall shape of the TED
2) the intensity and energy level of new structure in the TED due to the adsorbate
3) the effect of electric field and temperature on 1) and 2)

First let us examine in qualitative fashion the expectations of the above consideration for tunnel resonance. Based on the present physical picture (see Fig. 1) in which a Lorentzian shaped broadened vertical level in the

adsorbate is positioned at Δ (energy relative to the Fermi level), the TED with transmission resonance can be expressed crudely as

$$J_{t-r}(\epsilon) = J(\epsilon)\left[1 + T_{t-r}g_t(\epsilon \pm \Delta)\right] \qquad (1)$$

where T_{t-r} is a transmission coefficient of the order of 10 to 10^3 and $g_t(\epsilon \pm \Delta)$ is a shape factor (Lorentzian in nature) centered on Δ, where $\epsilon \pm \Delta \lesssim 0$ is the condition for structural effects on the TED. Virtual levels occuring above the Fermi level can only be detected if they can be shifted below the Fermi level by field effects. Thus the resonance peak will have a skewed Lorentzian shape centered on Δ. This shape results from the well-known broadening of the vertical adsorbate level as the atom approaches the surface due to overlap between the adsorbate virtual level wave function and the continuum of metal wave function near Δ. The expected functional form of $g_t(\epsilon \pm \Delta)$ is

$$g_t(\epsilon \pm \Delta) = \frac{1}{\pi(\epsilon + \Delta)^2 + \Gamma^2} \qquad (2)$$

where Γ is the half heighth width of the broadened adsorbate level. As shown by Bennet and Falicov[6] Γ increases sharply with decreasing metal-adsorbate distance.

A word or two concerning the magnitude of T_{t-r} should be given. Crudely speaking T_{t-r} is the ratio of the adsorbate coated to bare surface tunneling probability of the electrons at Δ where the adsorbate modifies the bare surface potential by the presence of the adsorbate potential well of width w and x_o from the surface. From WKB considerations of tunneling through a triangular barrier, the tunneling amplitude is proportional to $\exp\left[-c\int_{x1}^{x2}\left[\phi(x) - E_x\right]^{1/2} dx\right] = \exp\left[-c(E_f + \phi - E_x)^{3/2}/F\right]$. Assuming the adsorbate modifies the barrier by cutting out a square well of width w and height $E_x - Fx_o$, the qualitative expression for T_{t-r} becomes

$$T_{t-r} \tilde{=} F(\epsilon)\frac{\exp -c\left[(E_f + \phi - E_x)^{3/2}/F - (\phi - \epsilon_x - Fx_o)^{1/2}w\right]}{\exp\left[-c(E_f + \phi - E_x)^{3/2}/F\right]} \qquad (3)$$

$$\tilde{=} F(\epsilon)\exp\left[c(\phi - \epsilon_x - Fx_o)^{1/2}w\right]$$

where $c = 2\left[(2m)^{1/2}/\hbar\right]$. For $\phi = 4.5$, $E_x = -0.5$, $F \approx 0.3$ V/Å and $w = 2$ Å, $T_{t-r} \cong 18$. Also note that T_{t-r} increases as the well depth increases and that $J(\epsilon)$, the clean TED expression in eq (1) may be altered slightly by changes in the work function ϕ due to the adsorbate.

According to a highly simplified model[3] the virtual level Δ will shift downward with field F according to Fx_o. However, upon including the image potential term, polarization of the atom by the electric field and Stark shifts, a more complicated field shift of the resonance level may occur in practice. Assuming no temperature dependent change in the adsorbate position x_o, no particular effect of temperature on the tunnel resonance peak is expected.

Next, let us examine the effect of electron-phonon interactions on the tunneling electrons. Electrons tunneling from the metal at energy level ϵ inelastically scattered by a phonon excitation $h\nu$ will ultimately tunnel through a separate channel at $\epsilon - h\nu$ (see Fig. 2). Thus, the TED shape at the Fermi level will be replayed at $\epsilon - h\nu$ reduced by a transmission factor T_{e-p}. In this case the expression for the TED becomes

$$J_{e-p}(\epsilon) = J(\epsilon)(1 - T_{e-p}) + J(\epsilon + h\nu)\, T_{e-p} g_p(\epsilon + h\nu) \qquad (4)$$

where the first term represents the reduction in the unperturbed TED due to electrons which channel separately at $\epsilon - h\nu$. The factor $g_p(\epsilon + h\nu)$ represents the line shape broadening due to a possible finite continuum of phonon levels or lifetime broadening.

In general the shape of the TED structure due to electron phonon interactions will be a reduced replica of the unscattered TED at the Fermi level. A theoretical description of this has been given elsewhere[1,5] for the closely analogous tunnel diode configuration. If the transition is sharp the shape factor $g(\epsilon + h\nu)$ will be near unity and the leading edge shape of the electron-phonon transition will be due to the temperature or resolution broadening of the Fermi level electrons. Thus, TED structures due to e-p transitions should exhibit a leading edge which broadens with temperature.

A Stark splitting of the electron-phonon transitions can be envisioned in the case of degenerate vibrational,rotational or bending modes. However, a qualitative prediction as to the magnitude of such field effects on the electron-phonon interaction is not possible from the present theoretical status. At best the effect of field on e-p transitions is expected to be smaller than for tunnel resonance. This is born out by the results of Lambe and Jaklevic[1] which show that the tunnel electron spectra of complex molecules is strikingly similar to the corresponding field free infra-red spectra.

The magnitude of the electron-phonon interactions will obviously be proportional to the oscillator surface density as well as T_{e-p}. In general $T_{e-p} \propto \langle m | p_z | o \rangle$ where p_z is the dipole moment perpendicular to the surface and $\langle m | p_z | o \rangle$ is the matrix element coupling the ground vibrational state m = 0 to m. As pointed out by Lambe and Jaklevic[1] this technique may also be useful in detecting Raman spectra.

Finally, let us consider the electron-electron (e-e) interaction. Our focus here is upon the possibility of the tunneling electron to excite the adsorbate electrons in the upper filled molecular orbitals to low lying excited states as depicted in Fig. 3. Since the tunneling electrons have several volts of energy relative to the uppermost filled state of the ad-molecules, excitation to levels a few volts above the ground state is possible. Cross sections for π orbital electrons should be of the order of the molecular dimensions for the conjugated molecules being examined here.

Qualitatively speaking, the expression describing the TED structure due to e-e interactionsshould have the following form

$$J_{e-e}(\epsilon) = J(\epsilon)(1 - T_{e-e}) + J(\epsilon + h\nu) T_{e-e} g_e(\epsilon + h\nu) \qquad (5)$$

It will be noticed that the form and symbol meaning of Equation (5) are identical to Equation (4). The shape factor $g_e(\epsilon + h\nu)$ originates from the same considerations which led to Equation (2). We anticipate Γ to be rather small for deep lying levels since metal-adsorbate orbital overlap will be small. If Γ is sharp, i. e., $\Gamma < kT$ the shape of the Fermi level TED is simply replayed at $\epsilon - h\nu$ as in

the case of electron-phonon interaction. We therefore expect temperature broadening to be manifest in the e-e transition where $\Gamma \lesssim kT$.

The effect of field on the e-e peak position can not be ascertained from our present understanding; however, it will be proportional to the difference between the field shift in the ground and excited state levels. Stark shifts for these highly polarizable molecules are likely to be important.

From elementary considerations two Stark shifts can be identified for electronic transitions. In the case of a non-degenerate state one may observe a quadratic shift in an energy level E_g with field. From second order perturbation theory it can be shown that[7]

$$E_g = e^2F^2 \sum \frac{|Z|^2}{E^o_{1,m,n} - E^o_{1',m',n'}} \tag{6}$$

where $Z = \int \Psi_{nl} Z \Psi_{n'l'} dx$ and $E_{1,m,n,}$ is a quantized energy state. Only transitions between states for which $\Delta l = \pm 1$ and $\Delta m = 0$ are allowable for finite Z. The integral Z is roughly proportional to the square of the orbital size. It is actually the difference between the field shift of two levels E_g and E_g' that is observed in a transition. Further considerations show that E_g can be related to the polarizability a as follows:

$$E_g = \frac{eF^2 a}{2} \tag{7}$$

For $a = 50$ Å and $F = 0.3$ V/Å the value of $\Delta E_g/\Delta F \cong 0.5$ Å. Thus, the quadratic Stark shift will be quite small for even highly polarizable molecules.

A linear Stark shift arises from the action of an electric field on a degenerate energy level E_o. The energy level will then split into two levels given by

$$E_n = E_o \pm eF \quad |Z|_{12}$$

where $Z_{12} = \int U_1^* Z_{12} U_2 \, dx$. In essence Z_{12} is roughly the mean difference in atomic size in states 1 and 2. For the hydrogen atom one can show that $Z_{12} = 3a_o$, where a_o is the Bohr radius. Thus, for the hydrogen atom $\Delta E_n / \Delta F = 1.5$ Å. Clearly, the linear Stark effect expected to predominate from these elementary considerations.

By way of summary we can write the expression for elastic and inelastic scattering in terms of the excess TED current $R(\epsilon) = J_a(\epsilon)/J_c(\epsilon)$, where the subscripts a and c refer to with and without the adsorbate respectively. Noting that $J_c(\epsilon) = J_o f(\epsilon)\, e^{\epsilon/d}/d$, where $f(\epsilon)$ is the fermi function, we obtain in the case of tunnel resonance from Equations (1), (2) and (3)

$$R_{t-r}(\epsilon) \tilde{=} 1 + F(\epsilon) \frac{\exp\left[c \, (\phi - \epsilon - Fx_o)^{1/2} w \right]}{(\epsilon + \Delta)^2 + \Gamma^2} \qquad (8)$$

More exact considerations by Plummer, et. al., [8] show that $F(\epsilon) \tilde{=} 1$ and that an additional smaller interference term should be added to Equation (8).

For inelastic processes one obtains from Equations (4) or (5)

$$R_{e-p}(\epsilon) \tilde{=} (1 - T_{e-p}) + T_{e-p} g(\epsilon + h\nu)\, e^{h\nu/d} \frac{f(\epsilon + h\nu)}{f(\epsilon)} \qquad (9)$$

at $T \to 0$ the second term is zero for $\epsilon > -h\nu$ and equals unity for $\epsilon \ll -h\nu$. The same form as Equation (9) occurs for $R_{e-e}(\epsilon)$.

The shape of $R_{t-r}(\epsilon)$ is an asymmetrical Lorentzian curve centered near Δ. In contrast R_{e-p} and R_{e-e} is a sharp step function whose steepness depends on T and the broadening function $g(\epsilon + h\nu)$ and the fermi function $f(\epsilon)$ which turns on at $\epsilon \tilde{=} -h\nu$. Besides the shape differences between $R_{t-r}(\epsilon)$ and $R_{e-p}(\epsilon)$ one observes that $R_{t-r}(\epsilon) > R_{e-p}(\epsilon)$ at $\epsilon = 0$. This follows from the fact that in the case of inelastic scattering, electrons emitted at ϵ can appear at $\epsilon - h\nu$, thus, reducing the Fermi level emission. Another important observation is that T_{e-p} and T_{e-e} have no obvious dependence on the size of $h\nu$. That is to say, the tunneling probability to first order for electrons at $\epsilon - h\nu$ is the same as at ϵ.

EXPERIMENTAL

Experimental details of the van Oostrom analyzer employed in this work have been described elsewhere[4]. Because of the relative insensitivity of this analyzer to the tip position we found it to be more versatile than the concentric sphere design described previously.

In order to facilitate the data reduction a Princeton Applied Research HR-8 lock-in amplifier has been incorporated into the system. This instrument allows electronic differentiation of the probe current, that is dI/dV, to be accomplished. Briefly, a 1000 hz, signal is impressed on the probe current I by modulating the bias voltage with a 10 to 20 mV signal.

The output dI/dV is plotted vs V_{bias} on an x-y recorder. The derivative can be taken electronically for probe current levels above 5×10^{-12} A. In most cases the 300 msec integrator time constant selector of the HR-8 is used. This allows the V_{bias} sweep of $\sim$ 3V to be made in $\sim$ 30 sec.

Both pentacene and metal free phthalocyanine were thoroughly outgassed prior to being put into resistively heatable plantimum buckets. Controlled deposition of molecules onto the tip could therefore be accomplished. The presence of an individual molecule(s) in the probe area could be ascertained by noting the rise in probe current due to the adsorption of a molecule. By observing the pattern and electron current the adsorbed molecule could be positioned in the center of the probe by magnetic deflection. This was done more effectively in the case of the pentacene results. Frequently the molecule would change its emission characteristics during TED measurements or disappear by diffusion or desorption from the probe hole region.

From the present state of knowledge one cannot be sure each adsorption event concerns an individual molecule or a higher order conglomerate of molecules. Both pentacene and phthalocyanine are conjugated planar molecules. Pentacene is a linear chain of 5 fused benzene rings and contains only C-C and C-H bonds where each C atom is sp^3 hybridized. Phthalocyanine is a four-fold symmetrical molecule approximately 10 by 10 Å and pentacene is an oblong molecule roughly

4 by 12 Å.

It is well known that large organic molecules frequently produce characteristic molecular patterns when adsorbed on a field emitter. These molecular patterns are usually a single spot, a doublet or quadruplet set of spots. With our geometry the molecular pattern frequently incompassed the total probe area. This was particularly true with the pentacene results.

RESULTS

Phthalocyanine

Although the TED results of phthalocyanine on W and Mo have been previously reported[4], we shall summarize the pertinent results here. Figures 5 to 15 show TED spectra for phthalocyanine on various planes of W and Mo at 77°K. The experimental details have been discussed elsewhere[4]. For the most part phthalocyanine was deposited onto the tip at 77°K. Removal of the phthalocyanine was effected by thermal heating, thus the substrate surface was carbon contaminated for the most part.

By monitoring the emission current while the molecules of phthalocyanine were being deposited one could detect the deposition of a single molecule (assuming monomolecular vaporization) of phthalocyanine. Often the probe current was very noisy and erratic due to what appeared to be random steric changes in the adsorbate-substrate configuration. These steric changes of the adsorbate frequently altered the TED structure. The amplitude of a lower level noise current appeared to increase with temperature. Thus, lowering the temperature to 20°K (liq H_2) may reduce this undesirable noise problem.

It was observed that ΔI was not only a function of temperature but was also directly proportional to I. Careful studies showed that

$$\Delta I \propto I \tag{10}$$

This relationship suggests that the electrons which traverse the ad-molecule deposit energy in vibrational or other themal modes of the molecule.

The different TED curves shown in Figures 4 to 13 arise from separate depositions of phthalocyanine onto the substrate. Unfortunately the electron beam could not be easily deflected so as to position the probe hole over a single molecular spot in these results; thus, some of the difficulty in reproducing a given TED structure may have been due to two or more molecules with different steric configurations contributing to the total TED. This limitation was eliminated in the pentacene work reported below. A further complication possibly hindering reproducibility was the continuing carbonization of the surface due to thermal cracking of the phthalocyanine molecules during cleaning. This undesirable feature too was eliminated in the pentacene results by low temperature field evaporation cleaning of the surface.

In summarizing the phthalocyanine TED curves we have also plotted the shift in the peak relative to the Fermi peak as a function of applied field. In the caption we have included when available the ratio of the adsorbate to clean probe current increase I_a/I_c, the clean work function ϕ_c, the work function change $\Delta\phi$ and the change in the pre-exponential factor of the Fowler-Nordheim (FN) equation; that is

$$B = \ln A - \ln A_c$$

where A_c is the clean value.

We should hasten to point out that parameters obtained from FN analysis of I(V) data where TED structure is present must not be equated with their original physical meanings. For example, FN plots are frequently non-linear as shown in Figure 17 which pertains to the TED shown in Figure 16.

The TED curves have been replotted from the original data and normalized to put the peak maximum at unity. Clean TED's are shown in most cases for comparison purposes. Two TED's at different field strengths are plotted for comparison for each TED structure observed. The maximum number of new peaks observed in the TED structure due to adsorption was three.

Figure 14 summarizes the field shift of the various TED peaks with applied

electric field strength. Because of some uncertainty in calculating field strengths due to carbon contamination, some error may be contained in the exact relative positioning on the F axis. Generally speaking results on a given plane should have greater relative significance.

Figure 15 shows a result obtained only in a few cases in which a large emission peak was observed above the fermi level. In another instance, peaks occurred both at 900 mV above E_f and -575 mV below E_f. In the latter case the -575 mV peak was much smaller than the 900 mV one.

The two TED curves in Figure 7 are from two different depositions. The TED curves of Figures 12 and 13 are derived from the same deposition; apparently, the molecule underwent a spontaneous steric change which gave rise to another TED structure.

Pentacene

The pentacene results were obtained on a 310 W emitter which was cleaned by field evaporation. Subsequent removal of pentacene was carried out by field desorption so as not to alter the substrate surface through carburization. The pentacene was always deposited and the TED curves taken at 77°K. Noise problems were similar to the phthalocyanine studies.

The summary of the pentacene results are given in Figures 18-21. These results were all obtained from singlet molecular patterns. Of particular interest are the peaks in Figure 21 appearing nearly 3 V below the fermi level. Figure 22 summarizes the field shift of the peaks observed in the pentacene results. The results of investigating the temperature effect on the TED structure is shown in Figure 23. Unfortunately it is extremely difficult to measure the TED curves above 77°K because of excessive noise and irreversible changes in the TED structure. Figure 24 is a replot of the TED structure shown in Figure 20 for the purpose of illustrating an unusual increase in the Boltsman tail as the field is increased.

DISCUSSION

The first and foremost objective is to determine which of the three possible mechanisms discussed above are operative. Clearly, the direction of future work and utility of this technique as a surface spectrometer cannot be determined until a clearer idea of the mechanism is ascertained. Let us first consider the two possible mechanisms; inelastic or elastic scattering.

One of the important differences between elastic and inelastic processes occurs in the ratio of $J(\epsilon = \Delta \text{ or } h\nu)/J(\epsilon = 0)$. That is to say the amount of emission from the subsidiary peaks relative to the fermi level emission is different in the two processes. For inelastic transmission resonance we obtain from equation (1) to (3)

$$J(\Delta)/J(0) = \frac{e^{\Delta/d}(1 + e^{c(\phi - \Delta - Fx_o)1/2\,W})(\pi\Delta^2 + \Gamma^2)}{\Gamma^2(1 + e^{c(\phi - Fx_o)\,1/2W}} \quad \text{or for } \Delta < \phi - Fx_o$$

$$J(\Delta)/J(0) \simeq e^{\Delta/d}\left(\frac{\pi\Delta^2 + \Gamma^2}{\Gamma^2}\right) \tag{12}$$

Similar considerations lead to the following expression in the case of inelastic scattering

$$J(-h\nu)/J(0) = e^{-h\nu/d} + \frac{T}{1 - T}\, g(h\nu) \tag{13}$$

If we include the field shift of Δ or $h\nu$ in eqs. (12) and (13) by assuming a linear shift of the form

$$\Delta(F) = \pm\Delta_o - \alpha F$$
$$h\nu(F) = -h\nu_o - \beta F$$

and if we further note that $d = CF$, eqs (12) and (13) become

$$J(\Delta)/J(0) \simeq e^{\pm\Delta_o/CF - \alpha/C}\,\frac{\pi(\pm\Delta_o - \alpha F)^2 + \Gamma^2}{\Gamma^2} \tag{14}$$

and

$$J(h\nu)/J(0) \simeq e^{-h\nu_o/CF - \beta/C} + \frac{T}{1 + T}\, g(h\nu) \tag{15}$$

On the basis of eq. (15) we can deduce that $J(h\nu)/J(0)$ always increases with F. This effect may be small, however, if T is large. Also, $J(h\nu)/J(0) \gtrsim 1$ if $T \gtrsim 0.5$.

We should point out that $h\nu_o$ must always be negative (ie, the peak displacement is below the fermi level at F = 0).

In the case of elastic scattering $J(\Delta)/J(0)$ can either increase (if Δ_o is negative or below the fermi level) or decrease (if Δ_o is positive) with F. If Δ is negative, the value of $J(\Delta)/J(0)$ will generally be small, the order of unity or less. It should be emphasized that $J(\Delta)/J(0) \propto e^{\pm \Delta_o/CF}$ whereas $J(h\nu)/J(0) \propto e^{-h\nu_o/CF} + B$ where the constant B may be large compared to $e^{-h\nu_o/CF}$.

We should point out that the derivation of the above equations is based on the assumption that all the electrons entering the probe area pass through the molecule. In the event this assumption does not hold, the terms on the right hand side of equations (1), (4) and (5) must be multiplied by the appropriate fractional area. On the basis of the cross sectional area of the two molecules studied and the overall magnification, it follows that the projected molecular pattern should cover the probe area as observed.

The ratio of the subsidiary peak heights to that at the fermi level increases with F in the TED peaks of Figures 4 and 5 for pht. on Mo (110). Also the rate of shift in the peaks with field is relatively small. In addition the subsidiary peaks are the order of twice the height of the fermi level emission. These observations fit the expectations for the case of inelastic scattering.

There are two additional peaks which have small values of dE (Displ.)/dF. The TED curve in Figure 6 with dE/dF = 1 Å exhibits a $J(-h\nu)/J(0)$ which increases with F. Also the peaks in the Figure 7 curve with dE/dF = 0.5 Å has $J(-h\nu)/J(0) \cong$ const. independent of F. For the most part the peaks with small displacements and small dE/dF were found on the 110 plane of either W or Mo.

Unpublished studies of the fine structure associated with pht absorded in a tunnel diode by Lambe and Jaklevic shows structure in the 50 to 80 mV region. Higher energy transitions were not investigated. Infra-red studies show strong absorption in the 90 mV region and is attributed to a C-H bending mode. Several strong IR peaks are also observed in the 125 to 200 mV region. The TED peaks observed at 90 and 150 mV (at 0.35 V/Å) may well correspond to the IR vibronic

spectra. The TED peak at 250 mV (the middle peak of Figure 7) also has characteristics of an electron-phonon interaction, but has no corresponding analogue in the IR spectra.

The leading edge of the pure electron-phonon interaction should possess a slope characteristic of the kT broadening at the fermi energy. However, additional broadening of the vibrational levels due to surface interactions or the applied field could lead to a less steep leading edge as observed for the middle peak in Figure 7.

The two TED curves shown in Figure 6 for pht on W (111) also exhibit small values of dE/dF, except for the lower energy transition which has a steeper portion segment. Both of these TED curves show ratios of J(hν or Δ) /J(0) which are nearly independent of F; this observation lends support to an electron-phonon description, i. e. equation (15) in which the second term is larger. The rather broad leading edge is somewhat puzzling to explain in terms of a strictly electron-phonon interaction. This particularly shaped TED was only observed for pht. on W(111).

As mentioned previously the middle peak in the TED curve of Figure 7 fits an electron-phonon interaction in view of the constant J(h ν)/J(0) independent of F and the small dE/dF. In contrast the high energy peak shifts markedly with F (i. e., large dE/dF) and J(h νor Δ)/J(0) diminishes with F. Thus, this peak is more in line with a tunnel resonance mechanism; that is eq (14) in which Δ_o is positive or above the fermi level. The relatively large value of I_a/I_c is also supportive of this explanation.

Figure 8 is another double peaked structure obtained from W(110) in which both peaks have the same shift with field and are separated by 400 mV. The relative positions of the peak heights vary only slightly with field strength. These observations including the relatively small value of I_a/I_c lend support for and electron-electron interaction. Conceivably, the double peak involves a combination electronic transition and vibrational overtone excitation. Interestingly, there is a strong IR absorption at 400 mV which corresponds to a N-H vibration.

The W(111) results of Figures 9 and 10 both have a large and identical value of dE/dF but are separated by 200 mV. The extremely large value of $I_a / I_c \approx 880$ and the rapid decrease of $J(h\nu \text{ or } \Delta)/J(0)$ with F lends support for a tunnel resonance mechanism. On this basis the very narrow half width reflects the narrowness of the virtual level of the adsorbate.

The TED curves of Figures 11 and 12 are from the same molecule which spontaneously changed its TED structure. We notice that in each case the lowest transition overlaps the fermi level emission at low fields. All peaks are strongly sensitive to field. Again the large value of I_a/I_c is indicative of a tunnel resonance mechanism. The separation of peaks in Figure 11 is $\sim$300 mV whereas in Figure 12 the separation is of the order of 200 mV. Here again it is possible that the lowest peak due to resonance tunneling while the higher transitions represent primary and overtone vibronic transitions.

The Figure 13 results show two peaks which have distinctly different field shifts. The relative peak heights are reasonably independent of field strength and the low energy transition has a broader half width. It is tempting to suggest that the two transitions are due to tunnel resonance and that the broader peaked low energy transition arises from overlap of the surface orbital with a nearby molecular orbital as suggested by the 2 Å slope of dE/dF. On the other hand the narrow half width high energy transition could be due to a spacially more distant molecular orbital as suggested by the 5 Å slope and correspondingly less overlap broadening of the adsorbate level. This interpretation does not correlate well with the field independent relative peak heights which according to eq (14), should vary exponentially with field unless Δ_o should fortuitously equal zero.

A summary of the field dependence of the peak positions in Figure 14 clearly shows 3 classes of relations. One group shows a large slope, between 3.9 to 5.0 Å; another group concentrates around the 2.0 Å slope, while the rest exhibit slopes less than 1 Å. Those in the latter group are best explained in terms of electron-phonon interactions as mentioned earlier. The group of peaks with the 3.9 to 5.0 and 2.0 Å slopes are either electron-electron or tunnel resonance

peaks. The parallel vertical displacements of many of the latter in some cases appear to be due to combination vibrational overtone transitions. In other cases a multiplicity of steric possibilities may alter the effective field strength and thereby cause horizontal displacements in the Figure 14 curves.

Striking evidence that some long lived excited states are involved in the pht. results is given in the Figure 15 results. Here a peak occurs 950 mV above and 1200 mV below the fermi level for F = 0.39 V/Å. This sort of result was observed only in a few cases of pht. depositions. In another result a peak was observed 575 above and 900 mV below the fermi level for F = 0.32 V/Å; however, the 575 mV peak was considerably smaller in this case. A possible explanation of these results is an Auger type mechanism in which an excited electronic state of the molecule is sufficiently long lived (compared to the interelectron tunneling time) that a subsequent tunneling electron stimulates the de-excitation. The latter electron is thereby given the de-excitation energy in the process and appears above the fermi level. The fact that the upper peak displacement from the fermi level is less the lower peak displacement by $\sim$ 250 mV may stem from the fact that stimulated de-excitation occurs to a metastable, rather than the ground state.

Figures 16 and 17 show a TED and a corresponding Fowler-Nordheim plot. In view of the non-linear nature of the plot one should exercise caution in attributing the usual physical significance to the Fowler-Nordheim constants.

Figures 18 to 21 are TED's obtained from various depositions of pentacene (pent) on W (310) at 77°K. These results were obtained from singlet molecular patterns. The results are similar to the pht. results except for the appearance of a peak at the astonishing displacement of $\sim$ 3 eV below the fermi level as observed in Figure 21. Excluding Figure 20 all the TED's exhibit relatively large peaks compared to the fermi level emission. For the most part the relative peak heights are independent of field strength, but the half widths become narrower with decreasing field strength as observed with the pht. results.

The Figure 18 results show three peaks, two of which show nearly identical field shifts. The upper peak exhibits a very broad half width and a small field

dependency and could best be ascribed to a tunnel resonance mechanism. The lower peak appears to be an electronic transition with a vibronic overtone.

The transitions observed in Figures 19-21 are also best explained in terms of an electron-electron interaction or tunnel resonance. The peak 3 eV below the fermi level in Figure 21 must be due to an electron-electron transition in view of the low tunneling probability for electrons 3 eV below the fermi level.

The summary of the pentacene results shown in Figure 22 show an interesting $\sim$ 150 mV separation between the 4 peaks observed with the 3.3 to 3.6 Å slope. As pointed out before, the vertical separation between these peaks is either due to a different true field at the molecule, or random spacial variations in the adsorbed state of the molecule which alter the electronic transition selection rules.

If one extrapolates to F = 0 the straight line curves of Figure 22 the 4 lower energy peaks all intersect the vertical axis above the fermi level. This should rule out an electron-electron mechanism since the energy exchange must be such that the tunneling electron loses energy. This would leave only a tunnel resonance mechanism to explain these results. In this case the vertical displacements could be attributed to steric effects which alter Δ.

As mentioned earlier elastic scattering due to tunnel resonance should be temperature independent in first order; whereas inelastic tunneling peaks should exhibit a temperature broadening of the leading edge. Figure 23 shows the results of an experimental attempt to examine the temperature effect on a TED peak due to pentacene. Many attempts were unsuccessful due to irreversible changes in the TED structure upon heating. Thus, the Figure 23 results, which should be taken as tentative until more results are obtained, show a definite broadening of the leading edge of the TED peak below the fermi level. This result then supports the electron-electron excitation explanation. The very large half width suggest an unusually large degree of broadening of the levels involved.

Figure 24 is simply a replot of the Figure 20 results on a semi-log graph to emphasize the unusual broadening of the leading edge as the field is increased. The degree of broadening corresponds to a few hundred degrees temperature

change. Since it is unlikely that the metallic electrons are heated even locally to such temperatures by emission heating, the broadening must be due to an electron-phonon interaction for electrons emitted at the fermi level. This sort of broadening was not a general occurrance.

SUMMARY

Both phthalocyanine and pentacene greatly alter the TED structure of W and Mo. A study of the temperature, shape and field dependence of the TED curves suggest that both electron-electron and electron-phonon interactions are involved. Elastic tunnel resonance cannot be ruled out as a possible mechanism in some results. Steric effects undoubtedly account for some of the apparent irreproducibility of the results; however, it is not yet clear to what extent steric or partial decomposition effects influence the TED results.

In order to give clearer understanding of the spectral information available by this technique we will complete the examination of pentacene and go to simpler molecules such as anthracene or benzene.

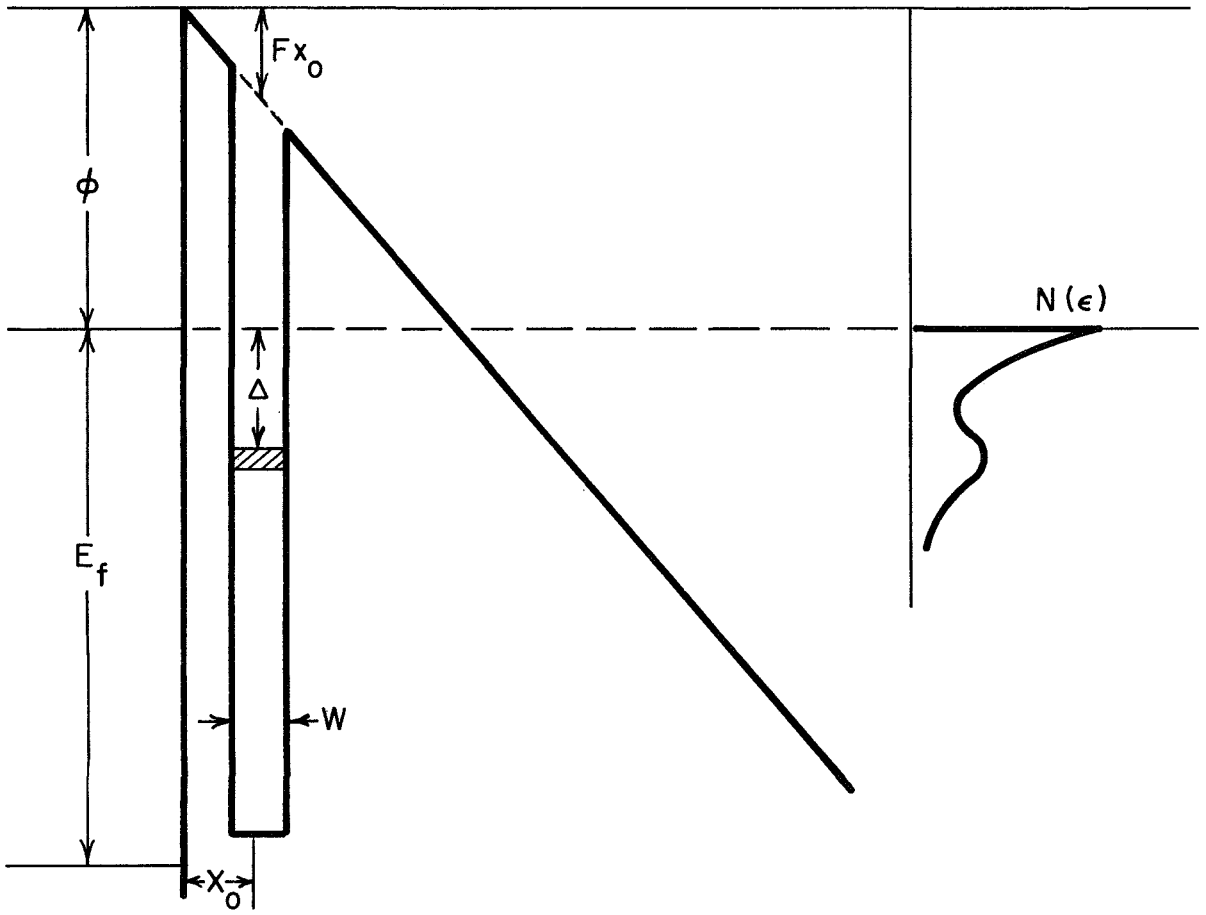

Figure 1 Electric potential energy diagram for tunnel resonance enhanced field emission.

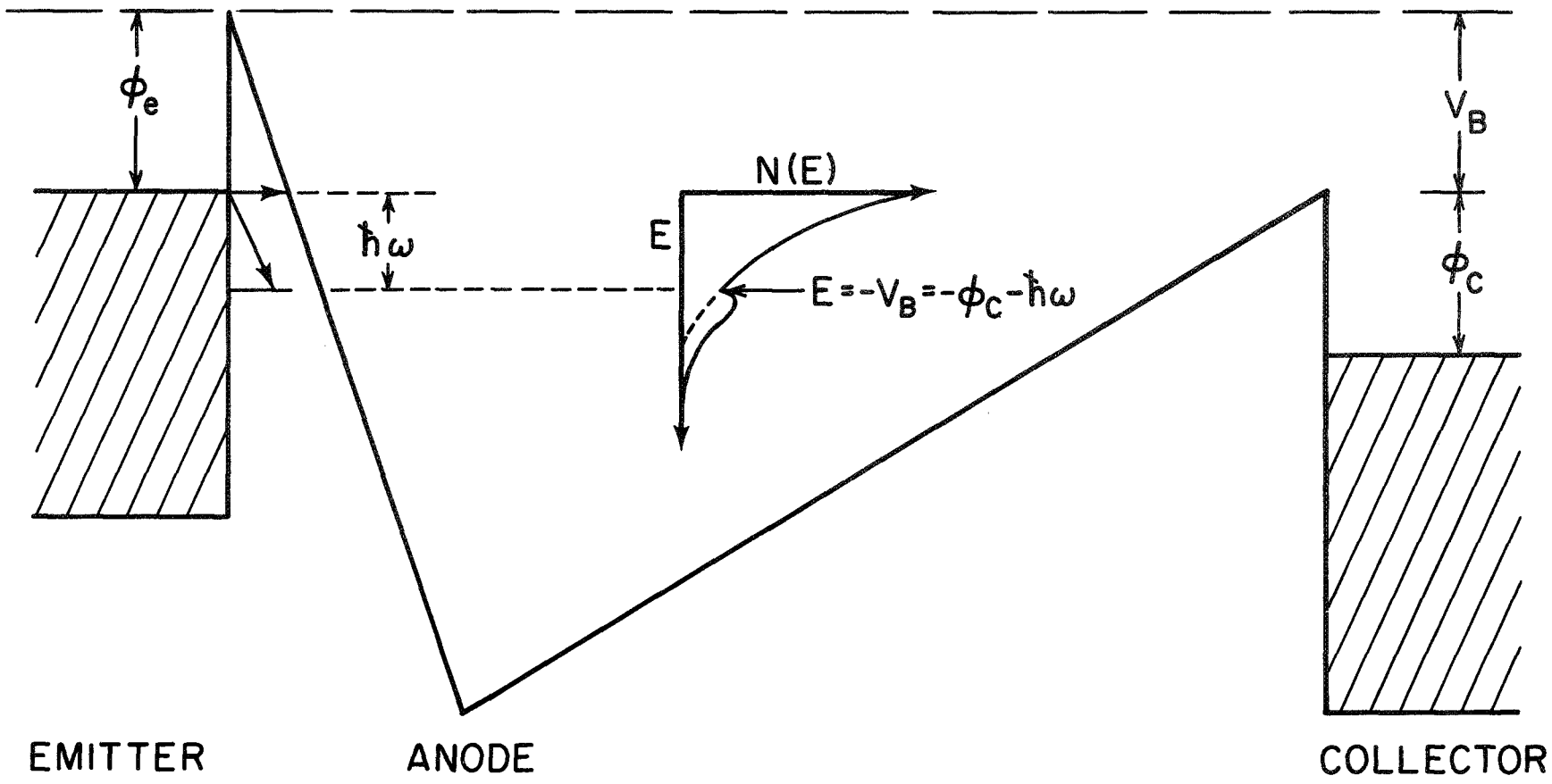

Figure 2 Electric potential energy diagram for electron-phonon interaction during field emission.

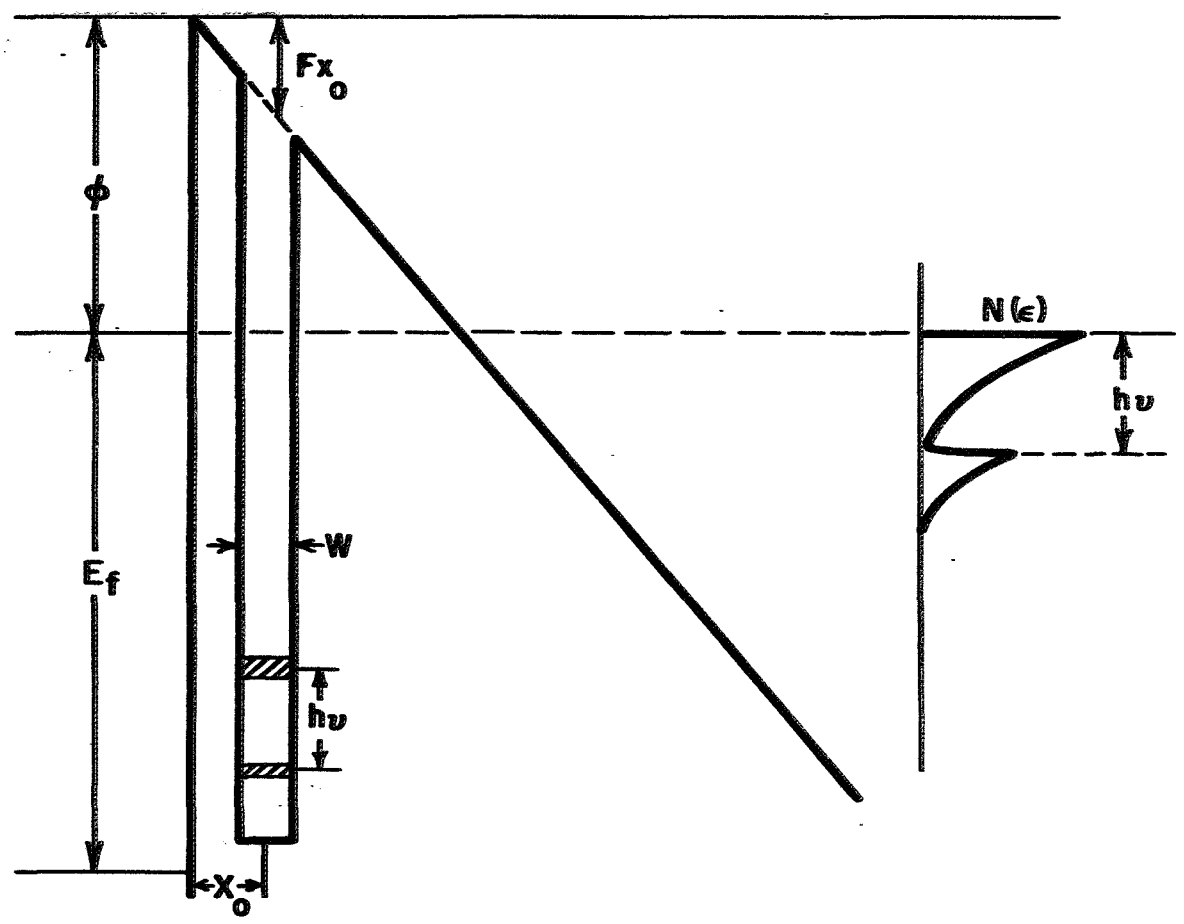

Figure 3 Electric potential energy diagram for electron-electron interaction during field emission.

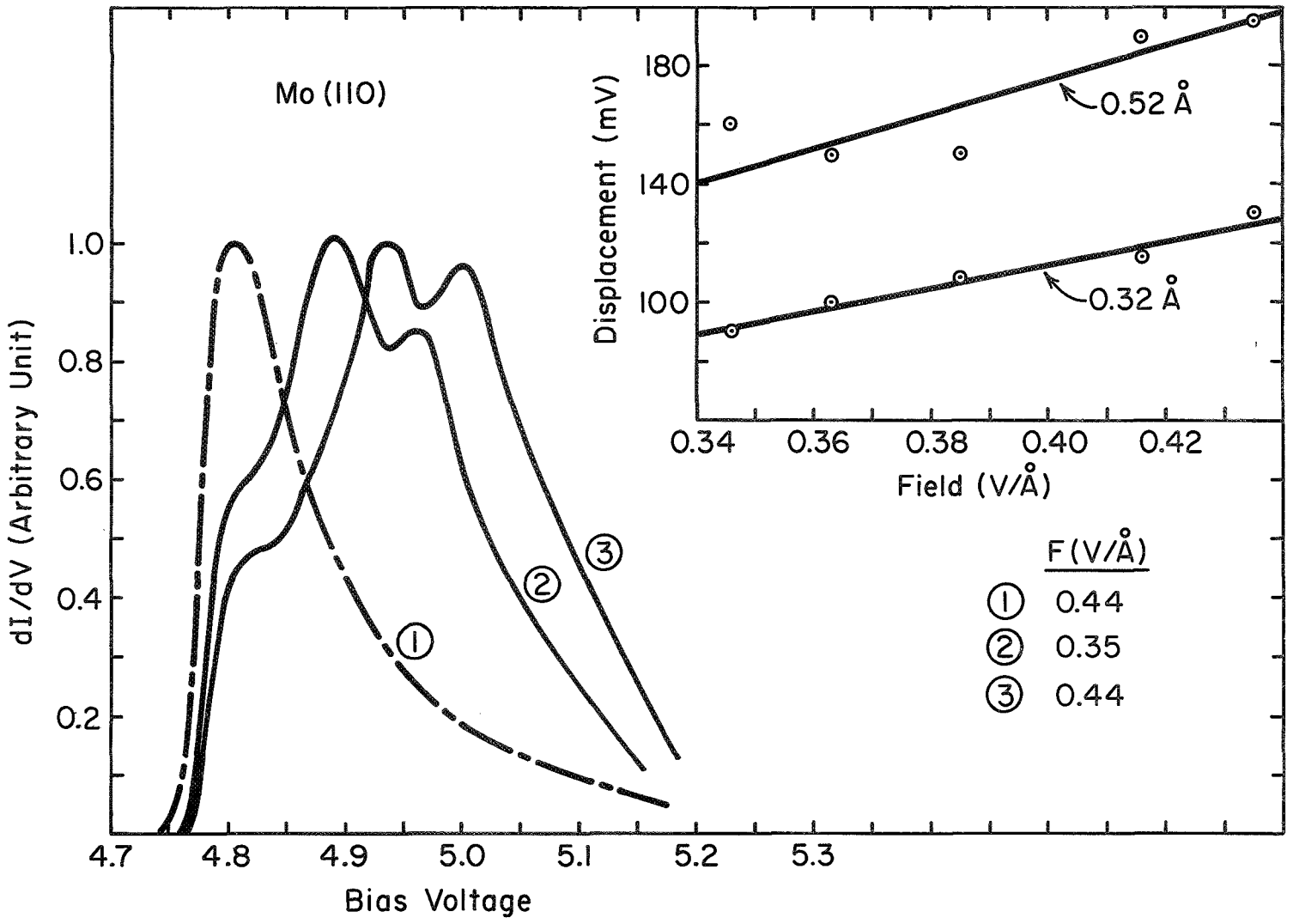

Figure 4 TED spectra for pht. on Mo (110); I_a/I_c = 27; curve 1 is clean TED.

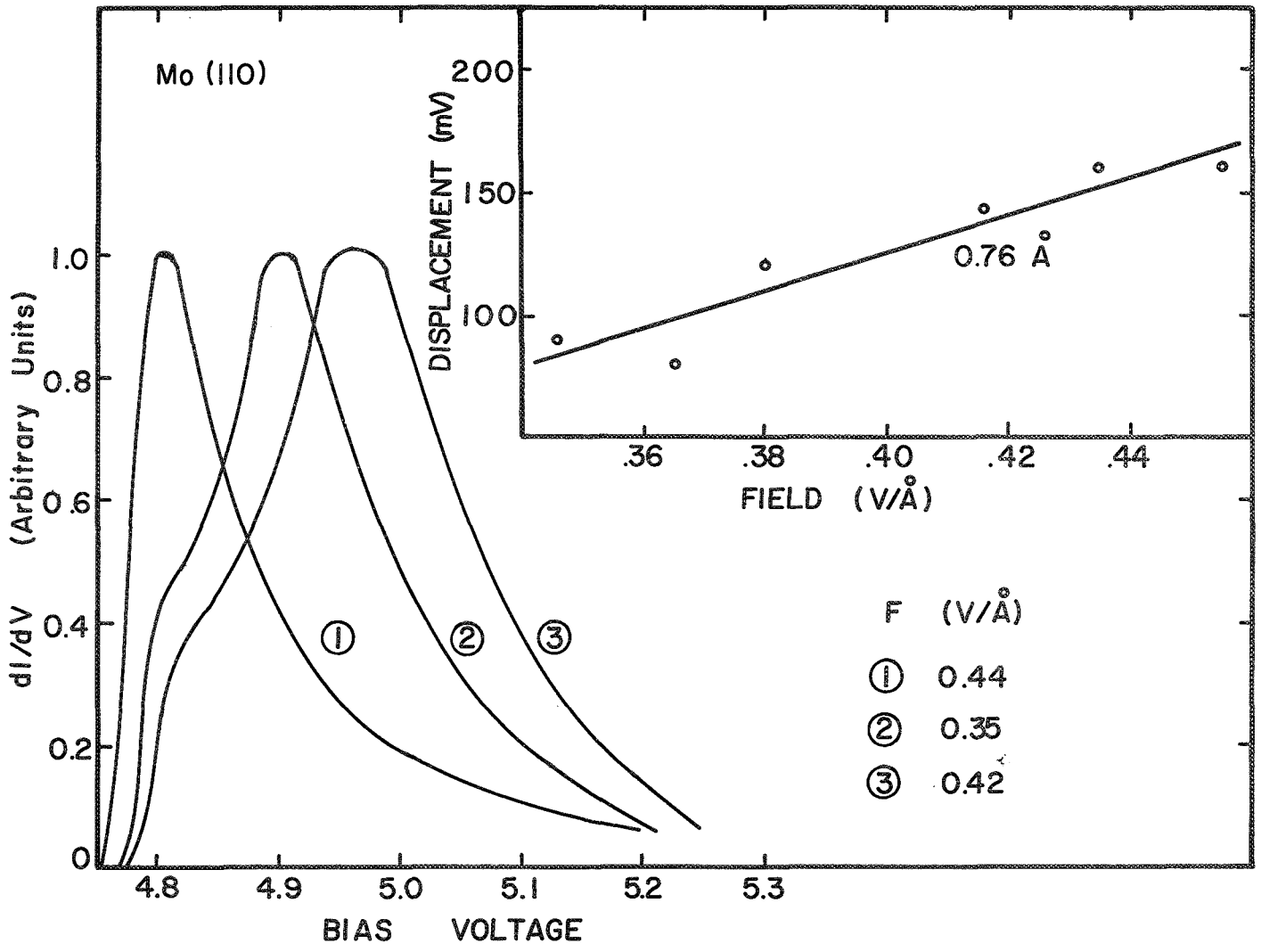

Figure 5 TED spectra for pht. on Mo (110); $I_a/I_c = 3.5$; curve 1 is clean TED.

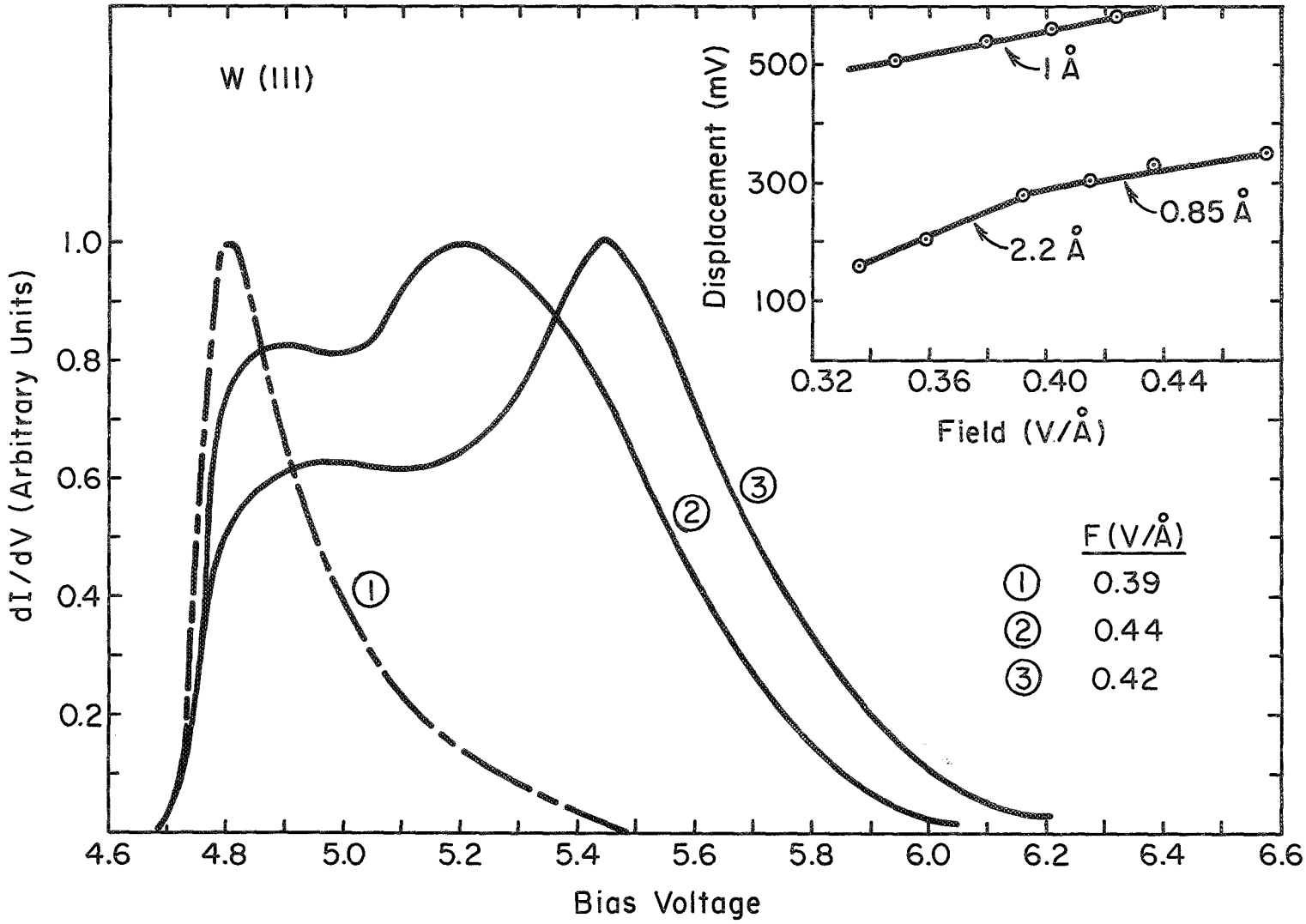

Figure 6 TED spectra for pht. on W (111); curve 1 is clean; curve 2, $\Delta\phi$ = -0.3 eV, B = 0.3, I_a/I_c = 2.7; curve 3, $\Delta\phi$ = -0.9 eV, B = -2.0, I_a/I_c = 4.2. Curves 2 and 3 represent two different depositions.

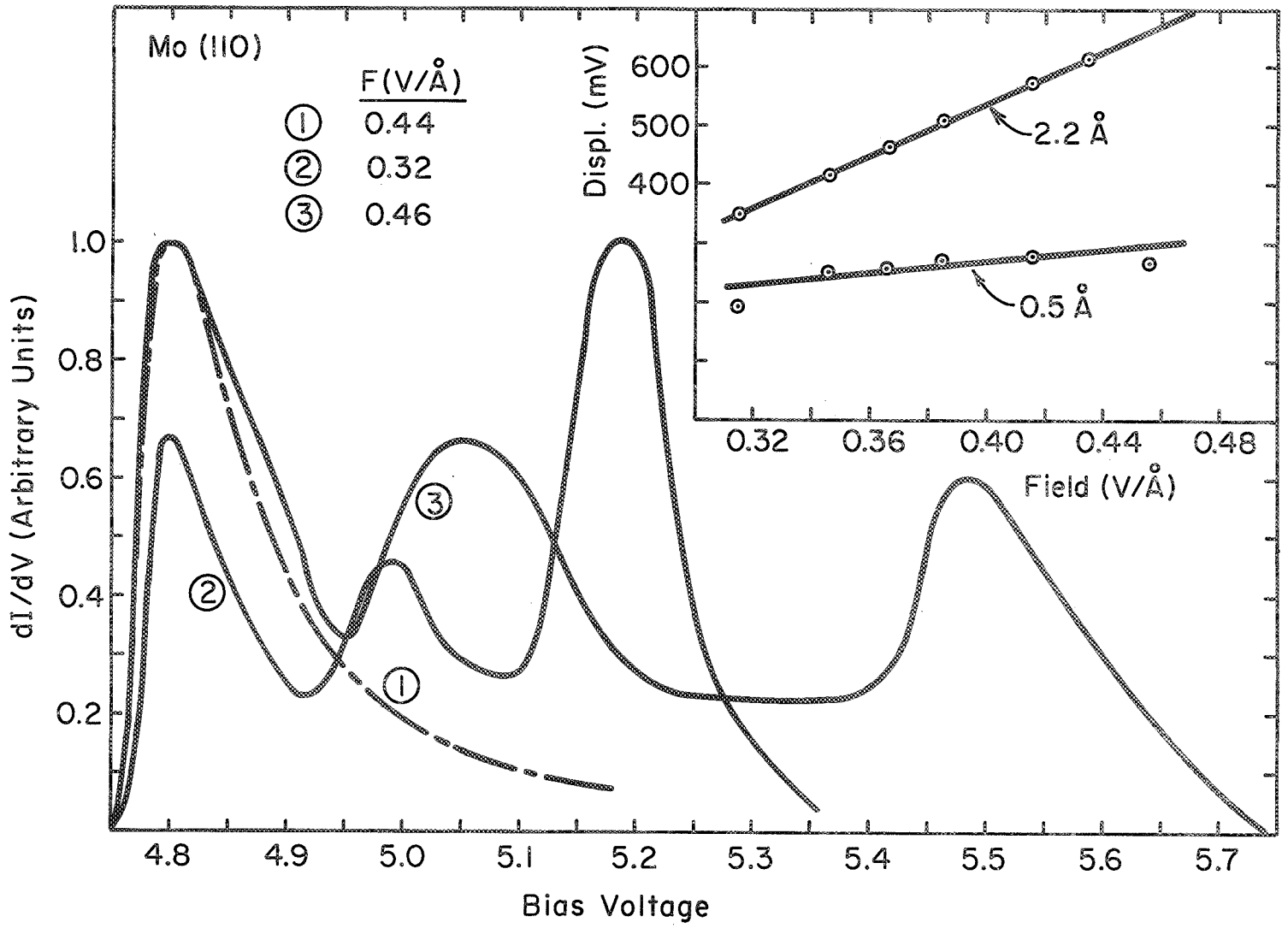

Figure 7 TED spectra for pht. on Mo (110); curve 1 is clean; $\Delta\phi \cong -0.48$ eV; $B \cong 0.4$; $I_a/I_c \cong 170$.

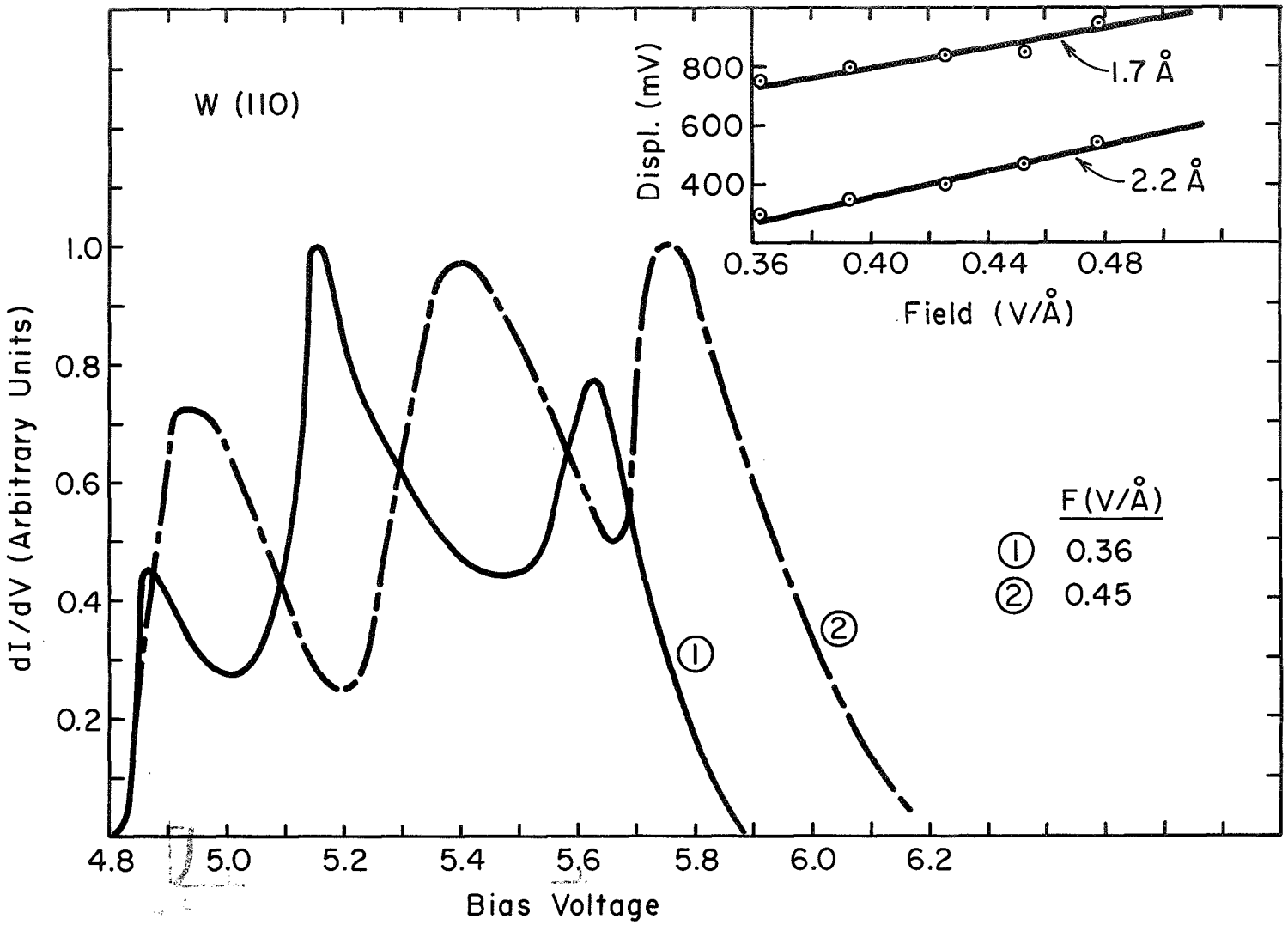

Figure 8 TED spectra for pht. on W (110); $\Delta\phi$ = 0.62 eV; B = -0.3; I_a/I_c = 25.

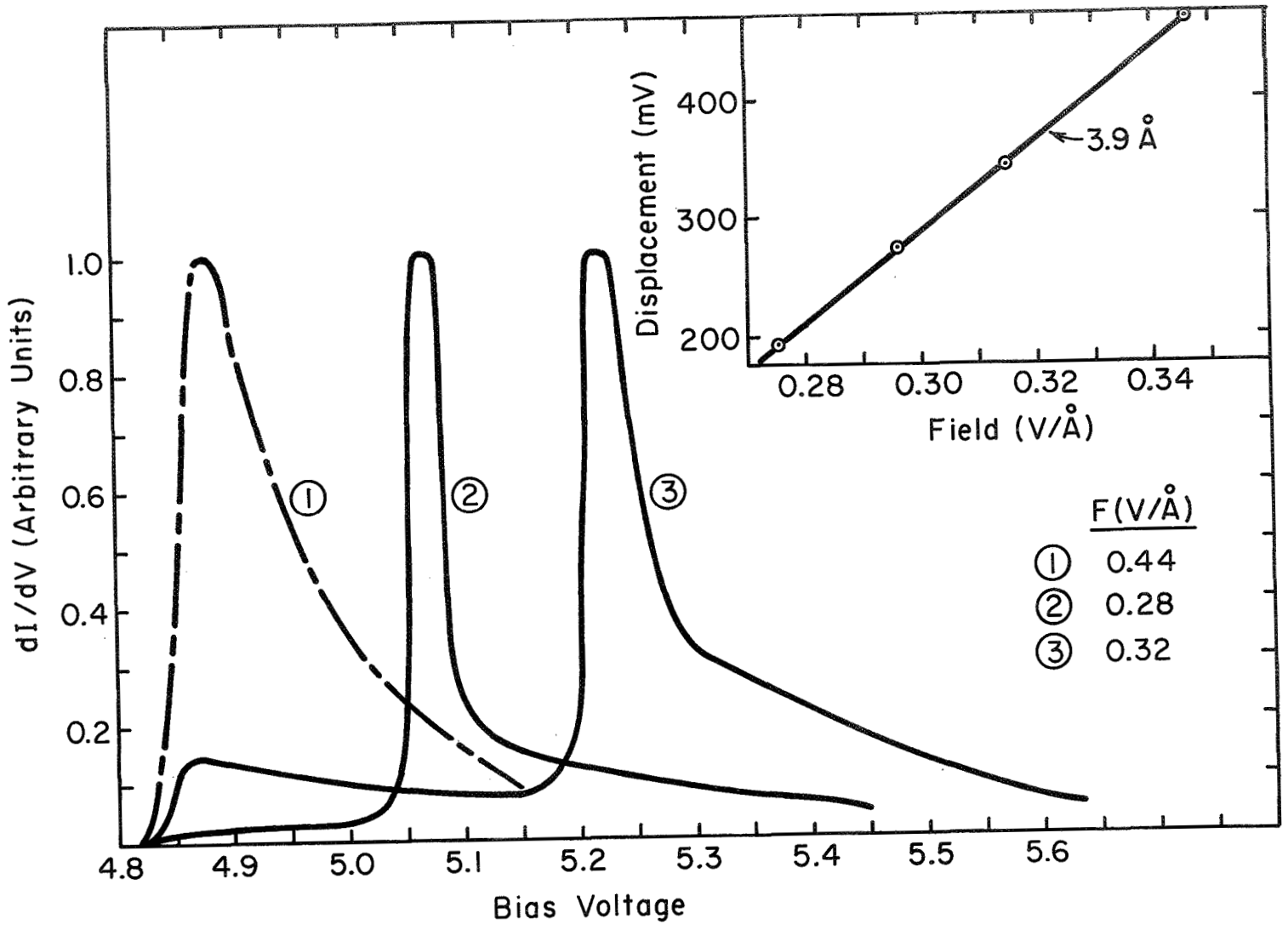

Figure 9 TED spectra for pht. on Mo (110); curve 1 is clean; $\Delta\phi$ = -1.0 eV; B = 1.0; I_a/I_c = 880.

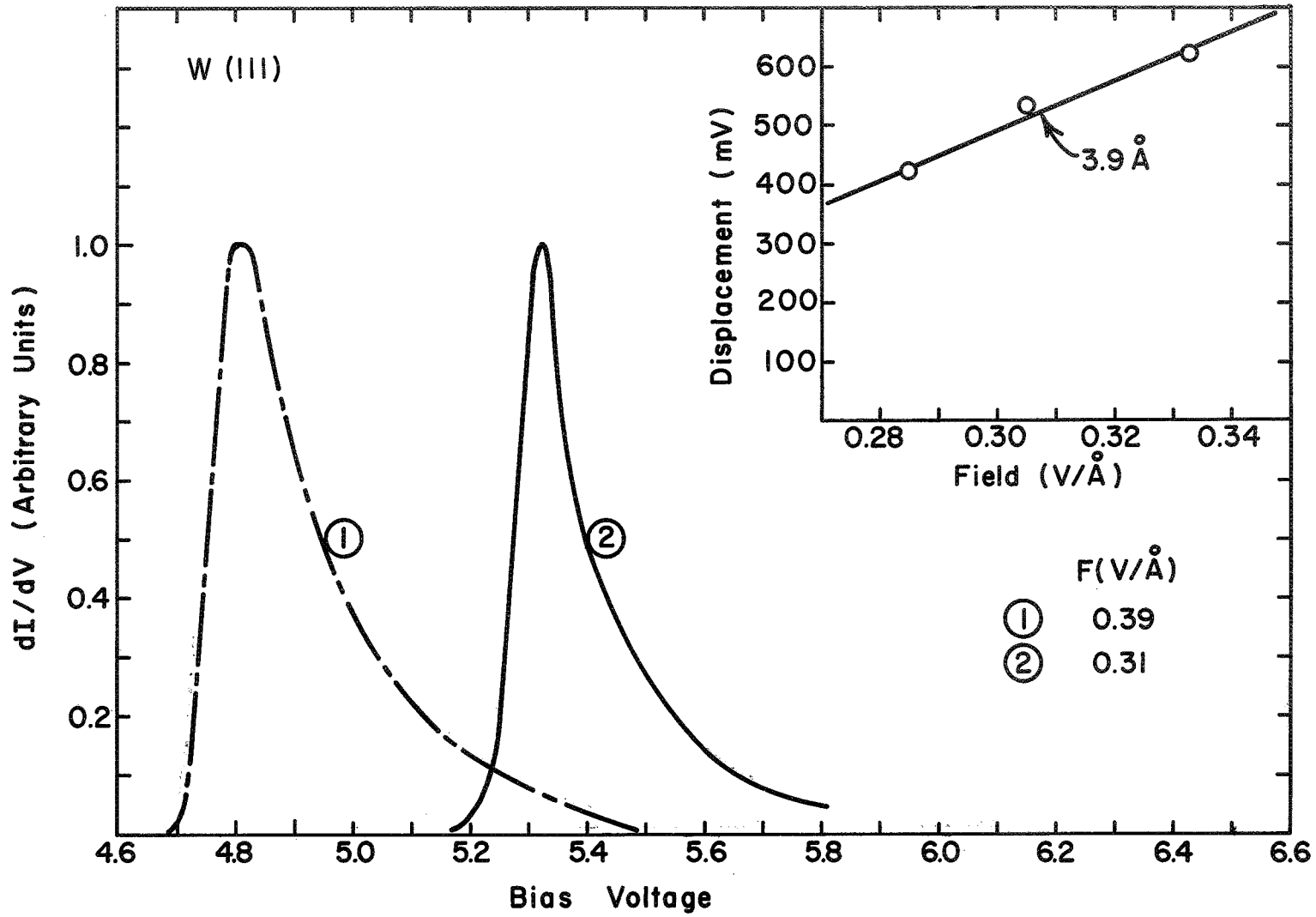

Figure 10 TED spectra for pht. on W (111); curve 1 is clean.

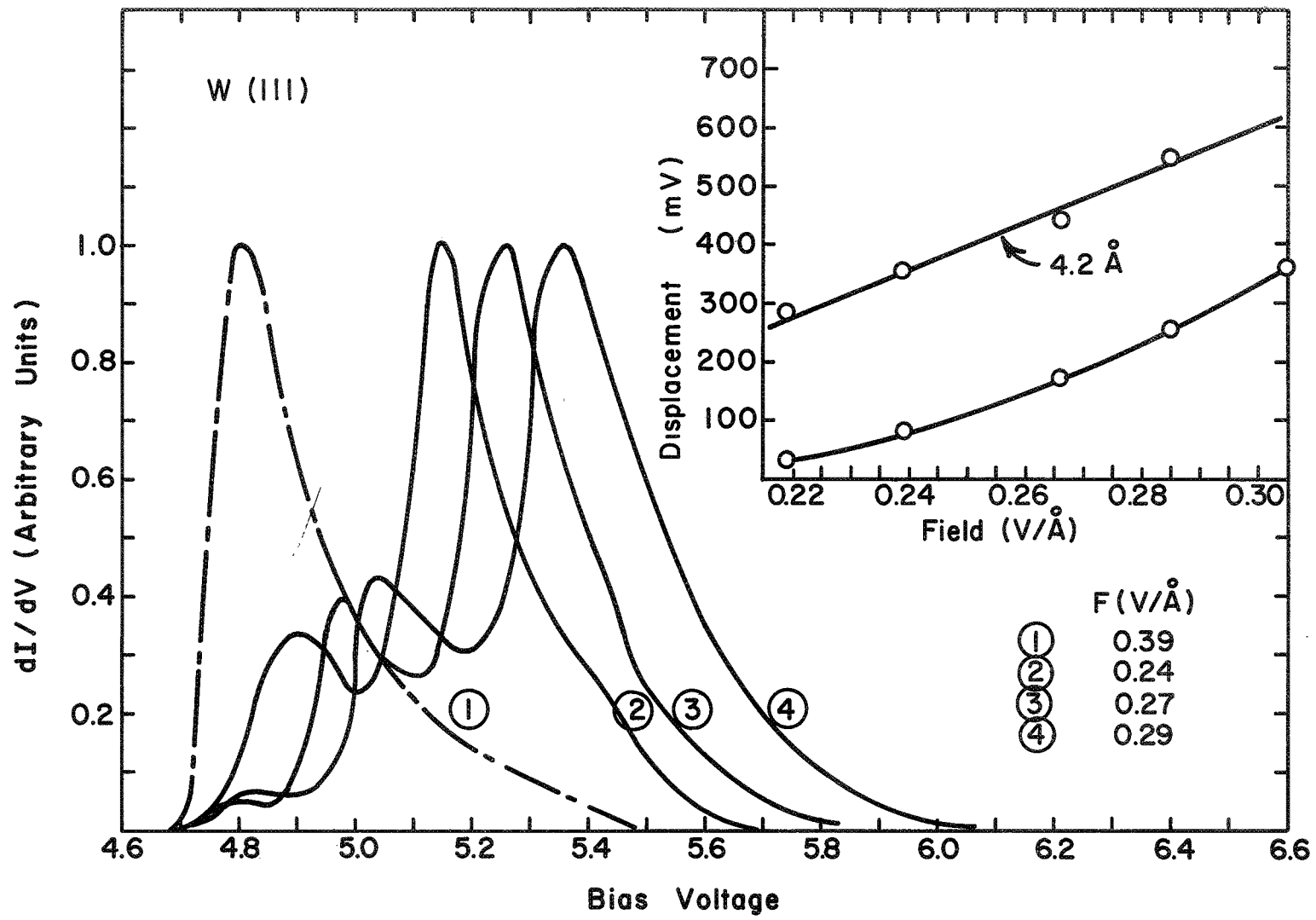

Figure 11 TED spectra for pht. on W (111); curve 1 is clean; $\Delta\phi$ = -1.3 eV, B = -0.8; I_a/I_c = 170

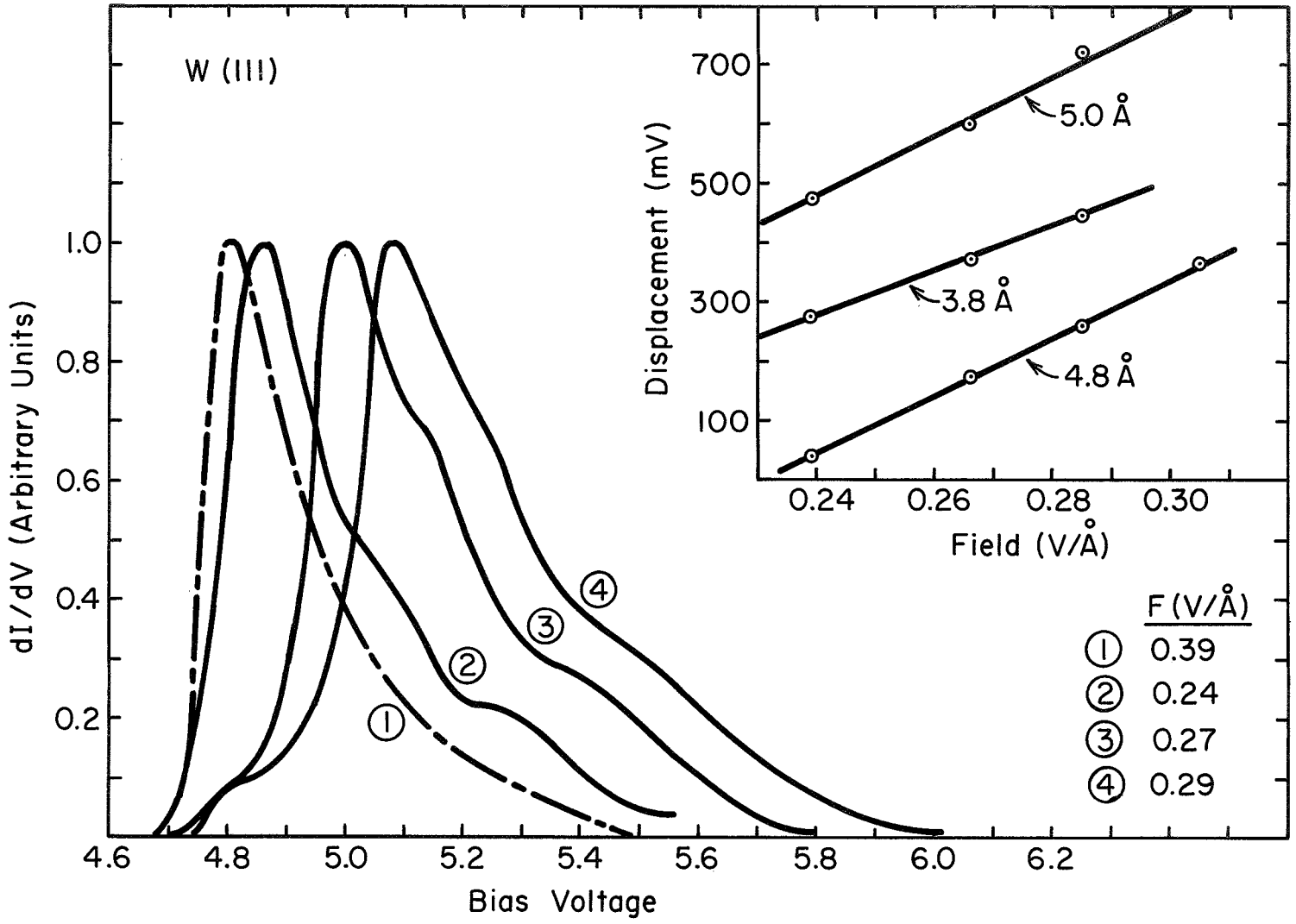

Figure 12 TED spectra for pht. on W (111); curve 1 is clean.

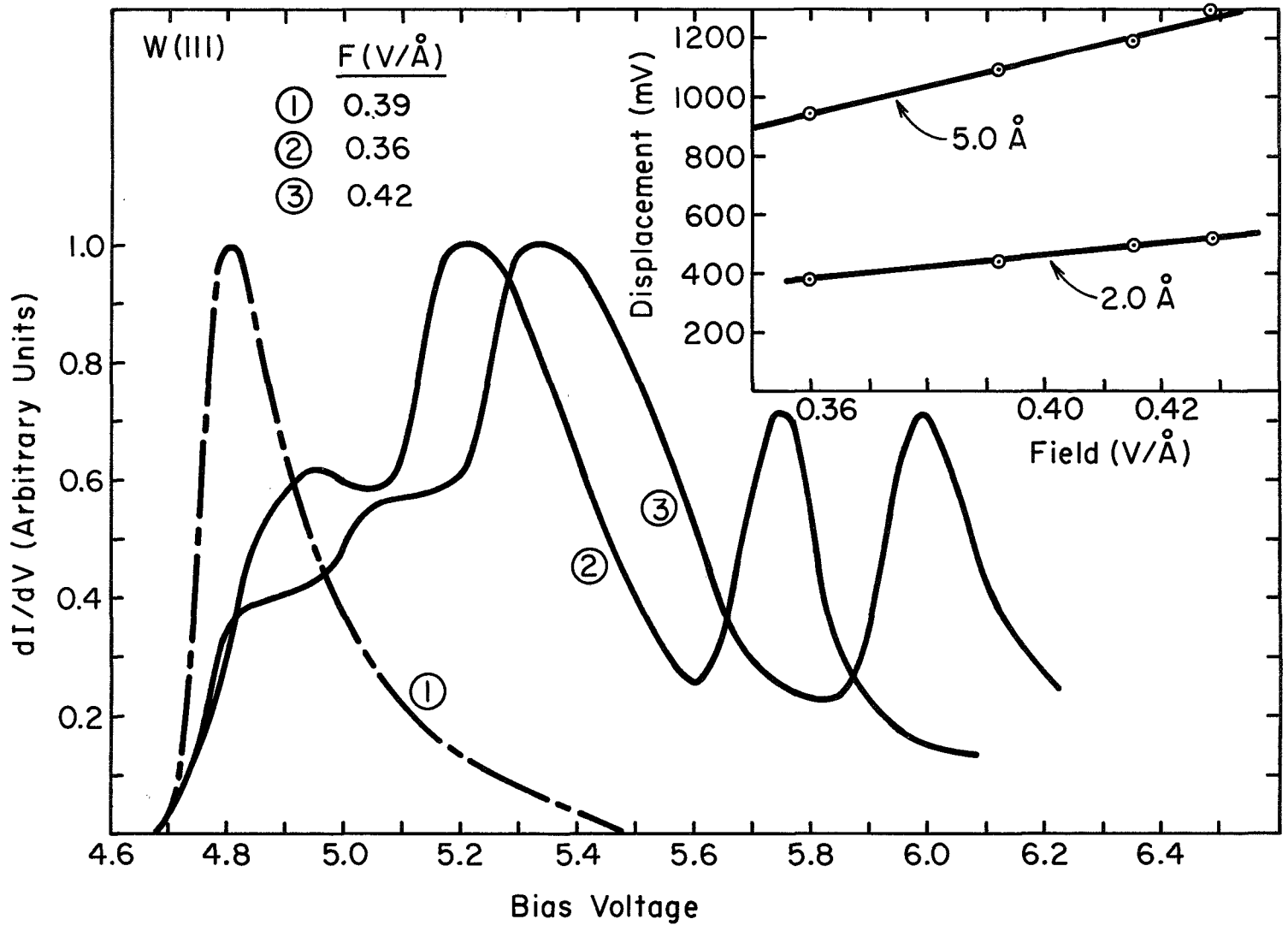

Figure 13 TED spectra for pht. on W (111); curve 1 is clean; $\Delta\phi$ = 0.83 eV; B = -1.0; I_a/I_c = 12.7.

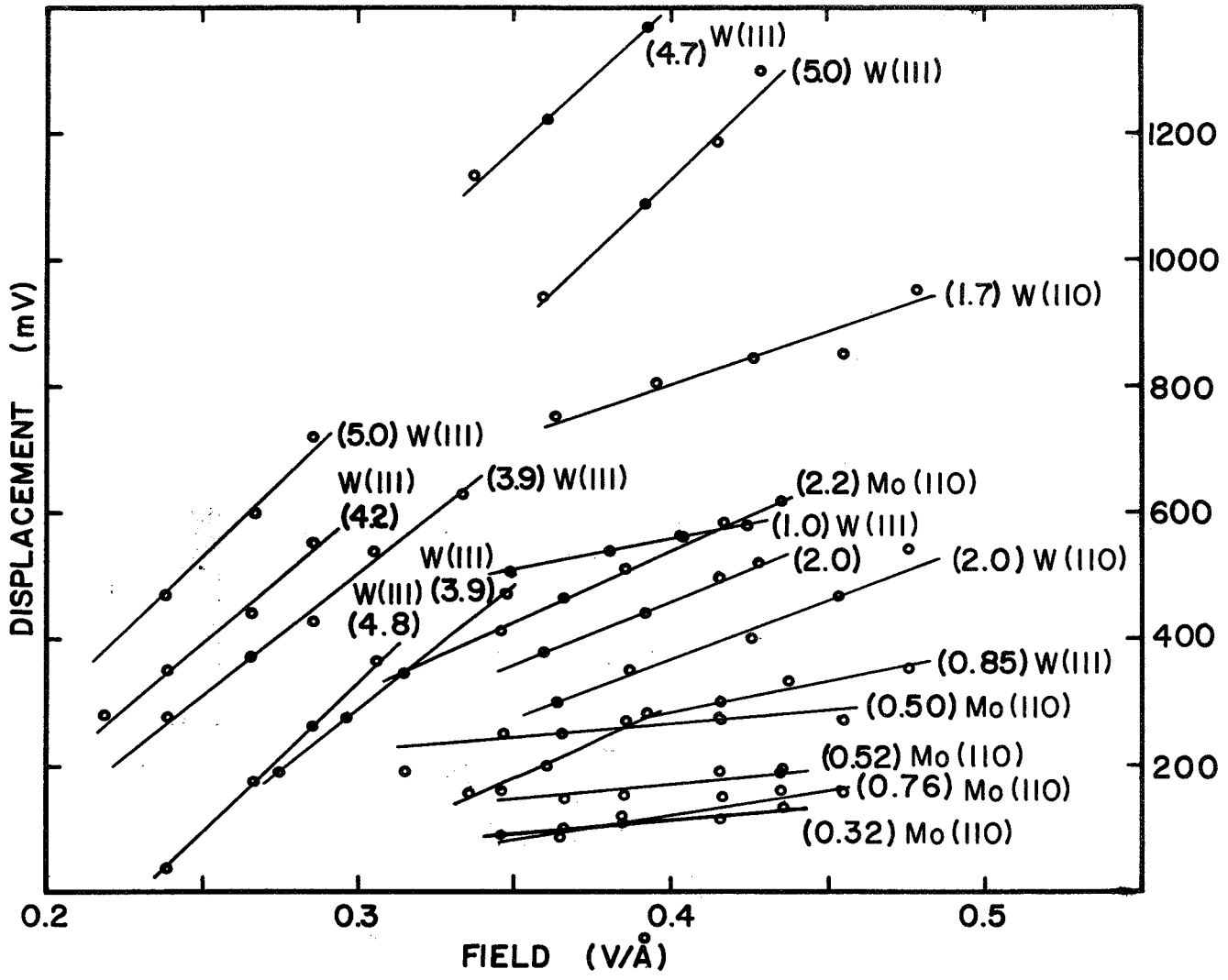

Figure 14 Summary of peak displacements vs field strength for pht. on various crystal faces.

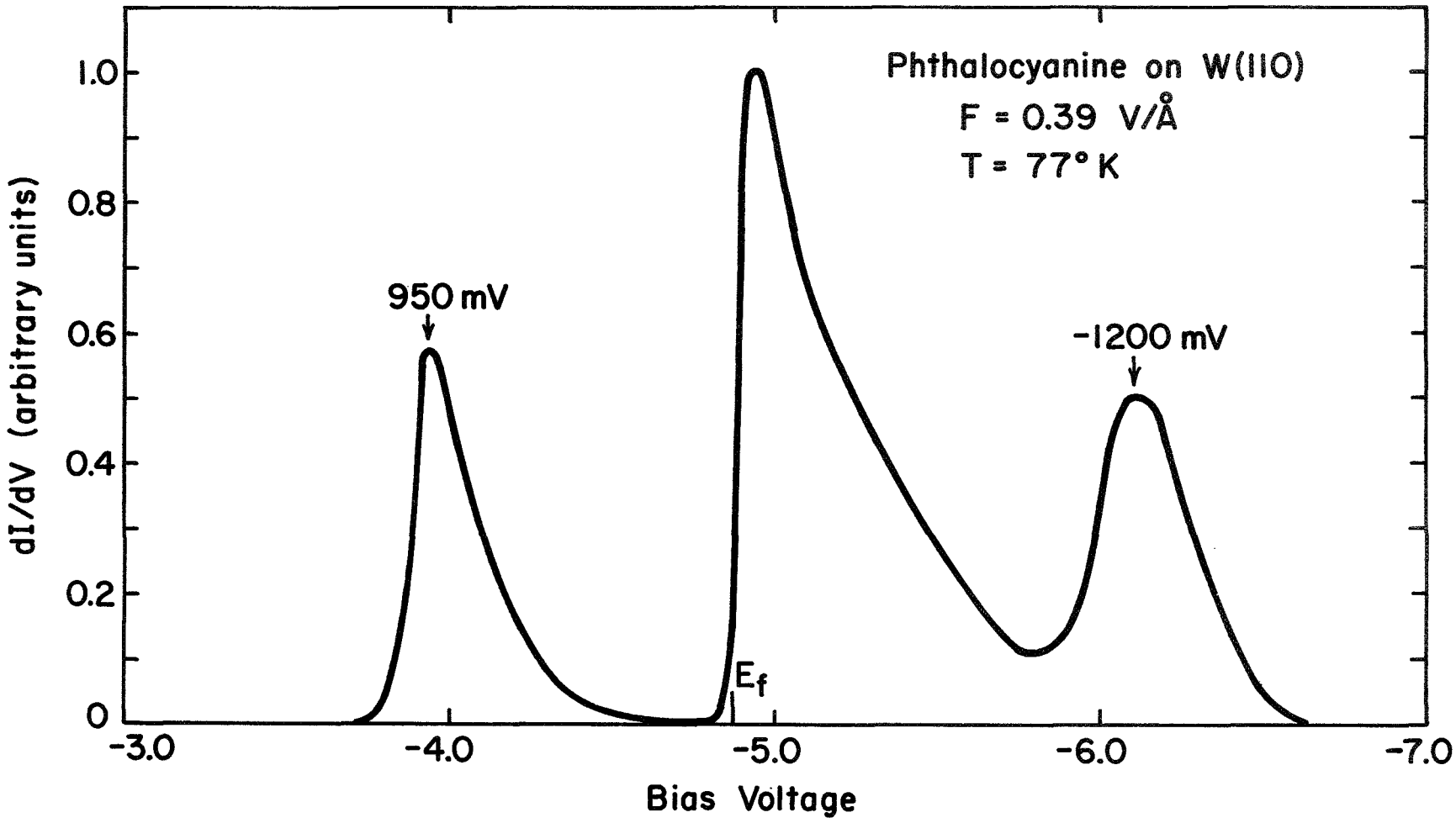

Figure 15 TED spectra pht. on W (110); I_a/I_c = 540. Note the peak 950 mV above the fermi level.

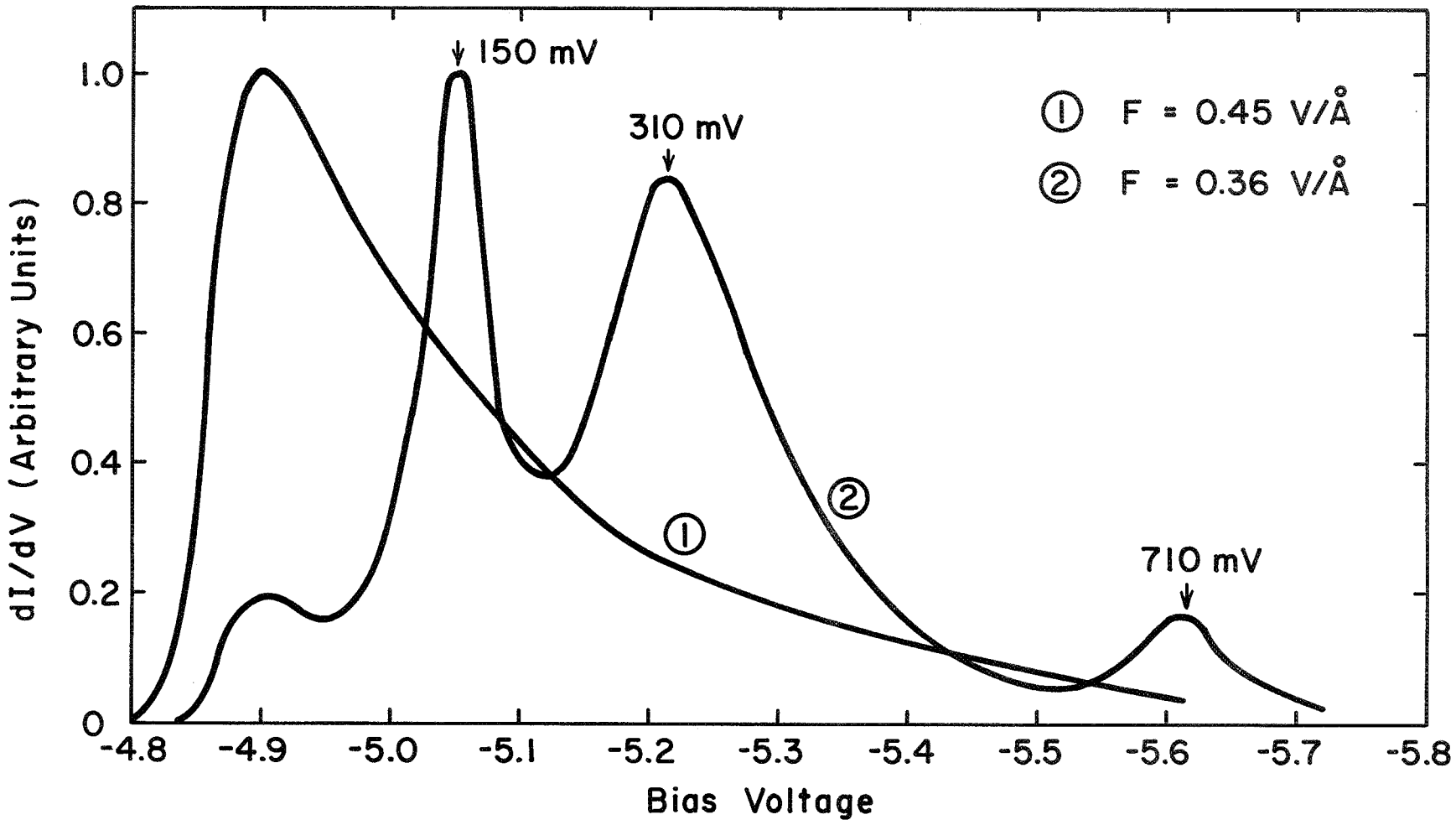

Figure 16 TED spectra pht. on W (110); I_a/I_c = 55. Note three distinct peaks.

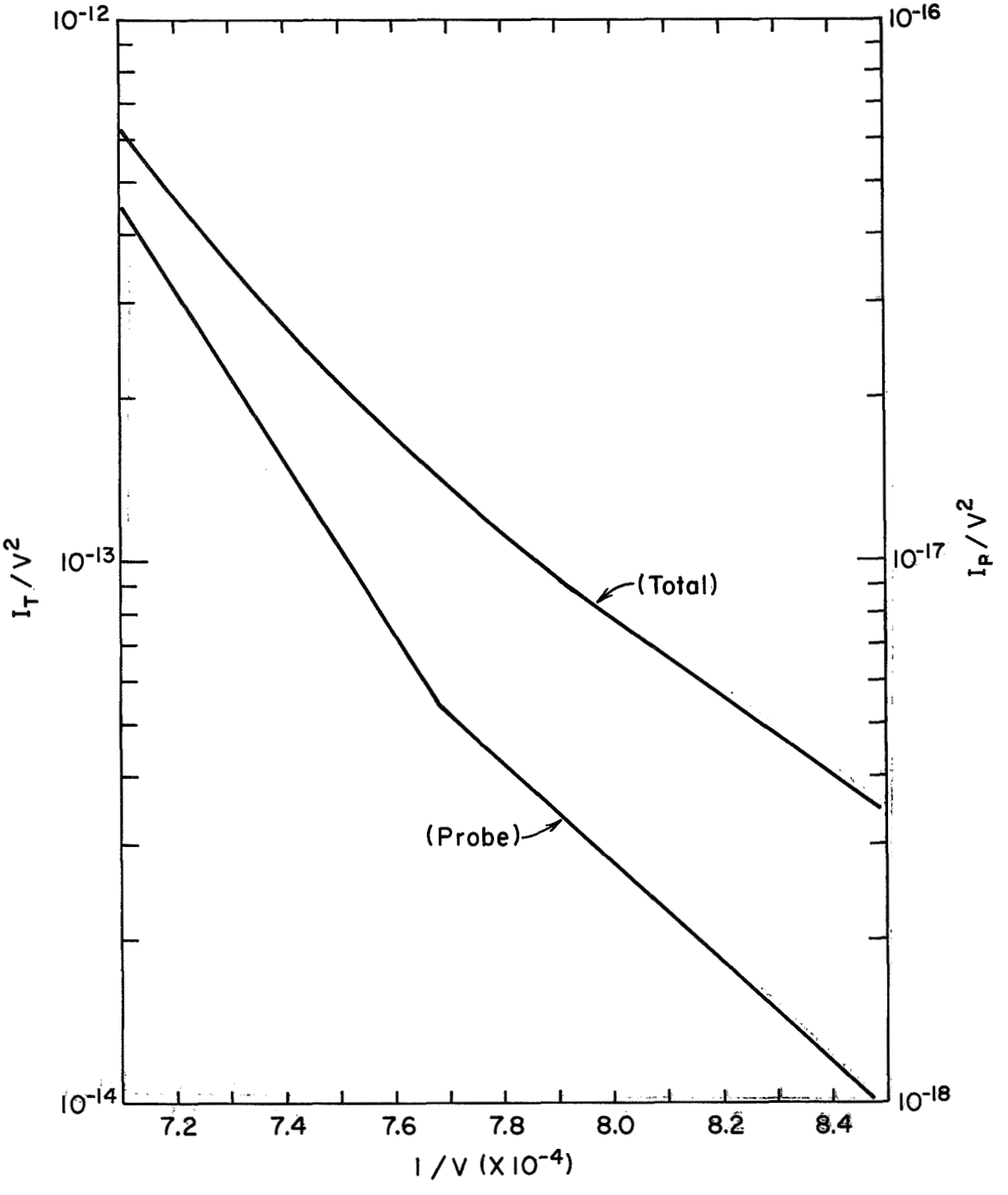

Figure 17 Fowler-Nordheim plot of probe and total current obtained from the TED corresponding to the Figure 16.

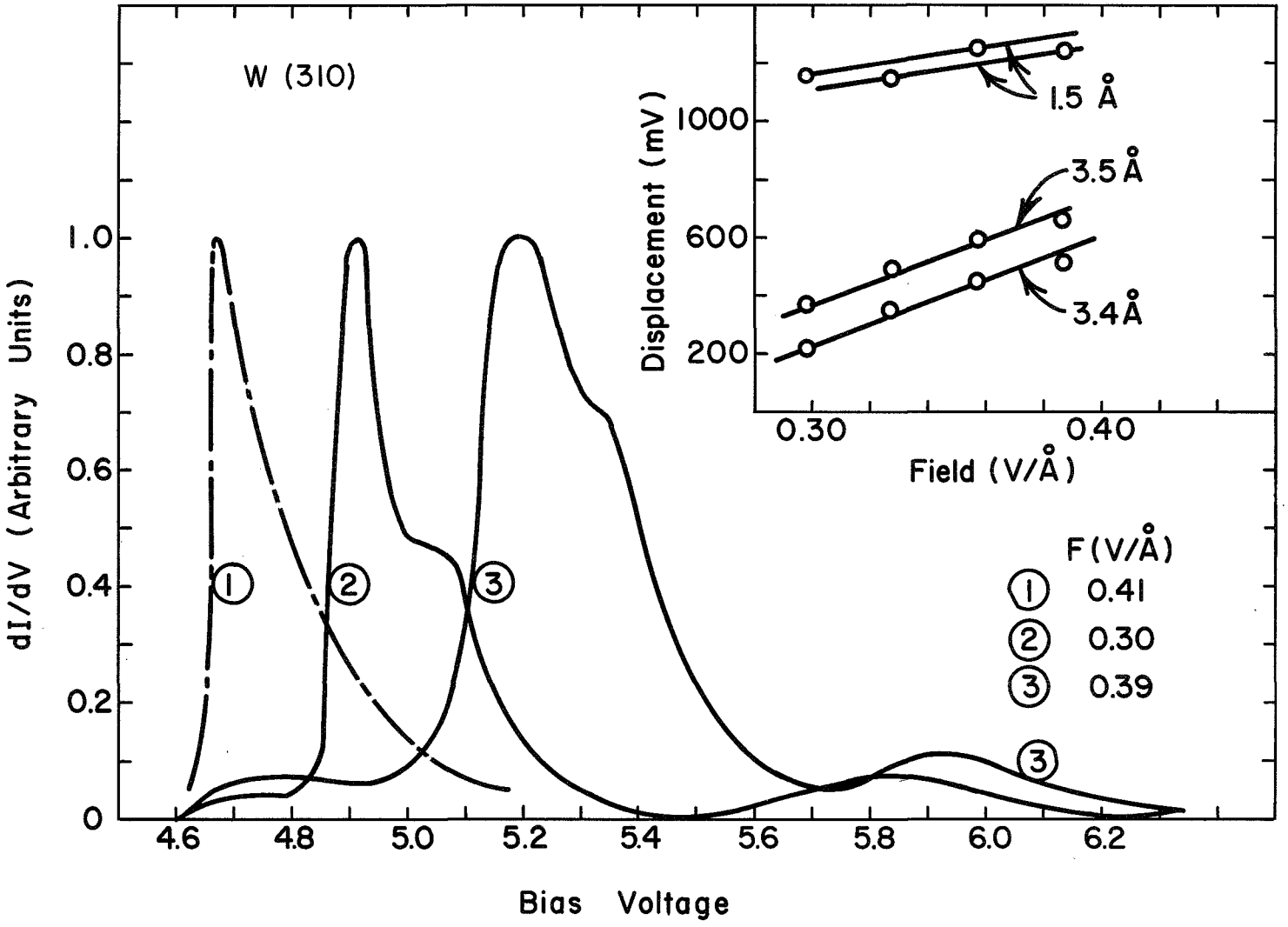

Figure 18 TED spectra pentacene on W (310); curve 1 is clean, $\Delta\phi$ = -1.7 eV, B = 2.0; I_a/I_c = 680.

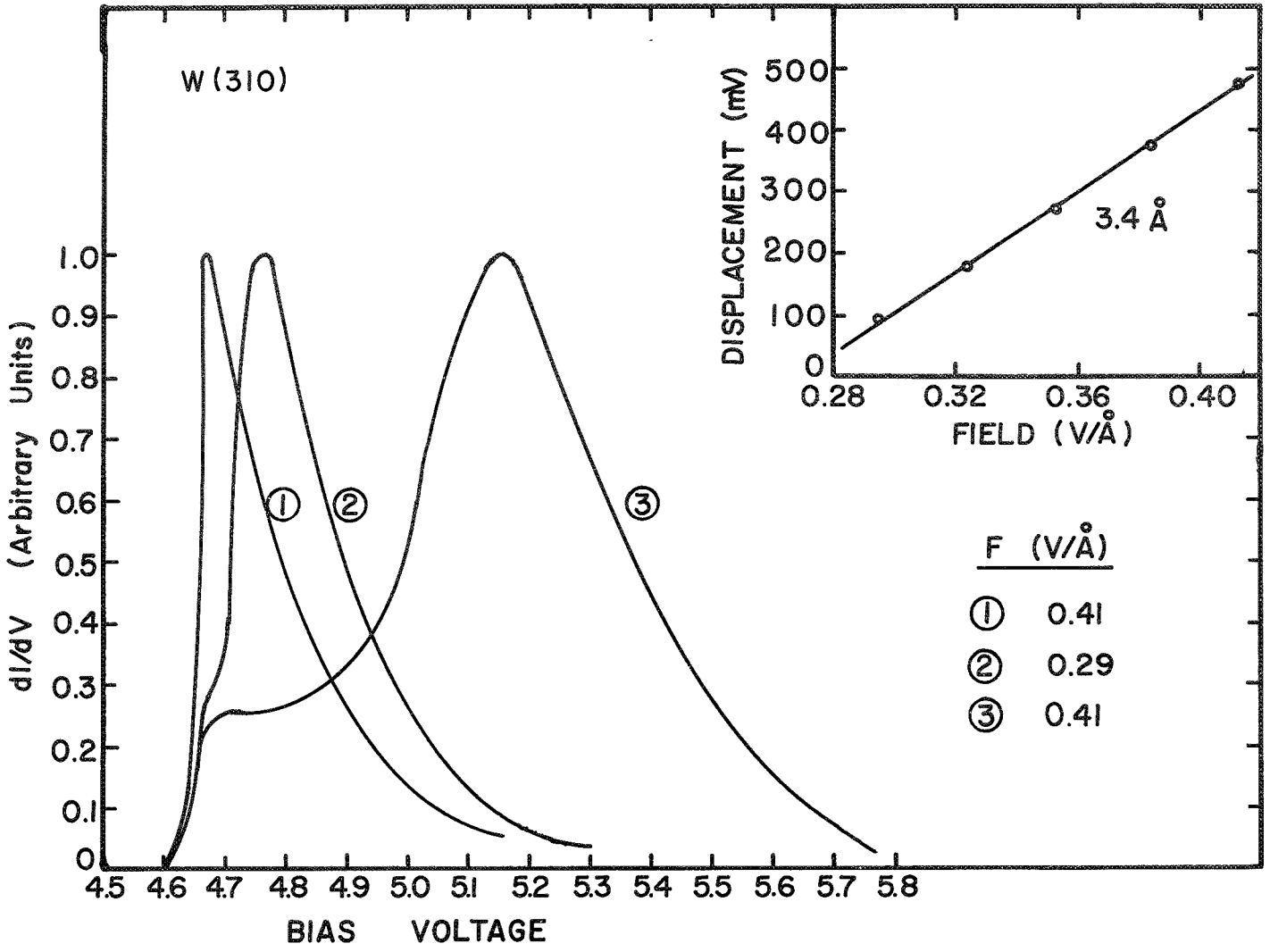

Figure 19 TED spectra pentacene on W (310); curve 1 is clean; $I_a/I_c = 55$.

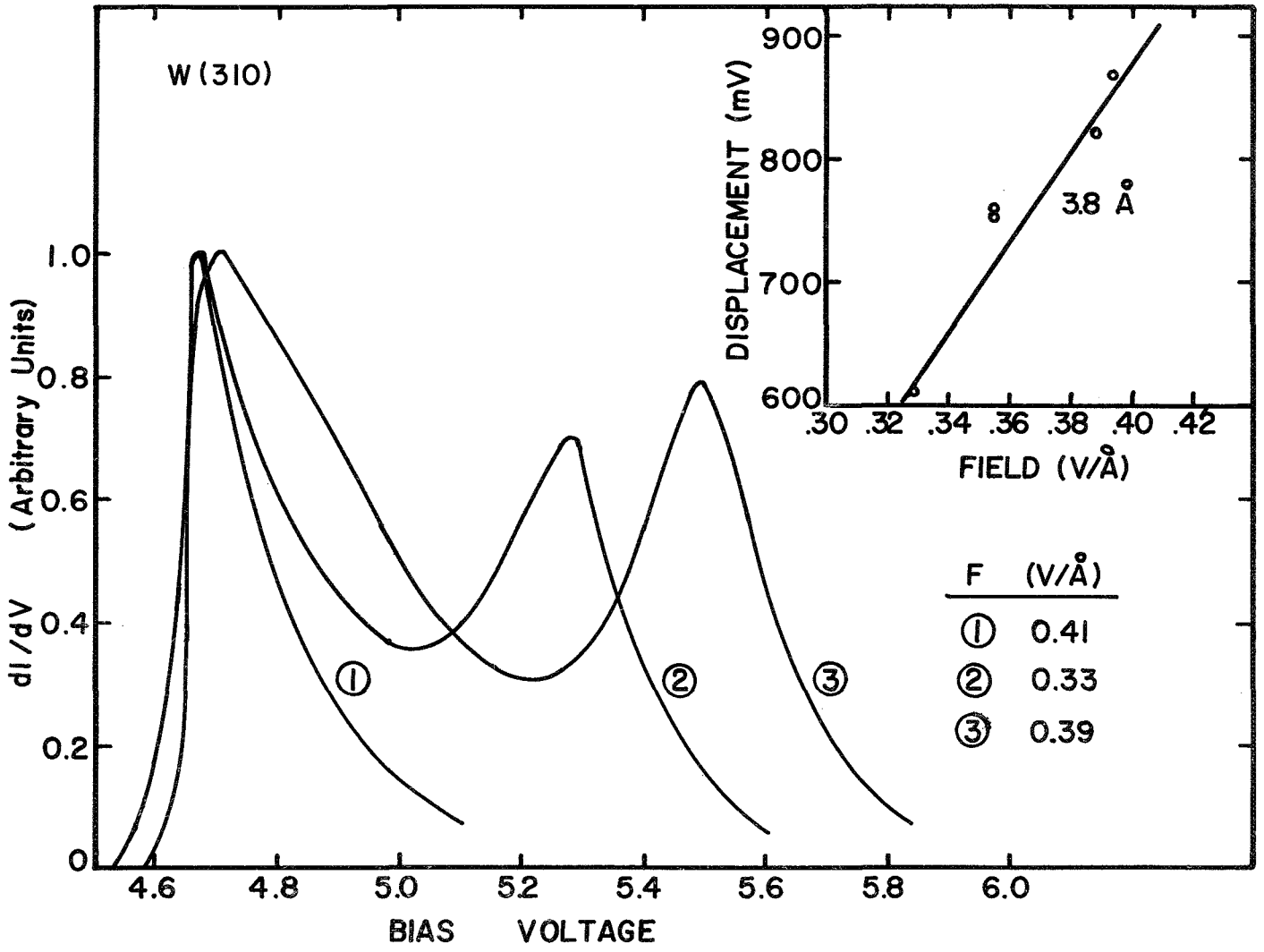

Figure 20 TED spectra pentacene on W (310); curve 1 is clean; I_a/I_c = 2.1.

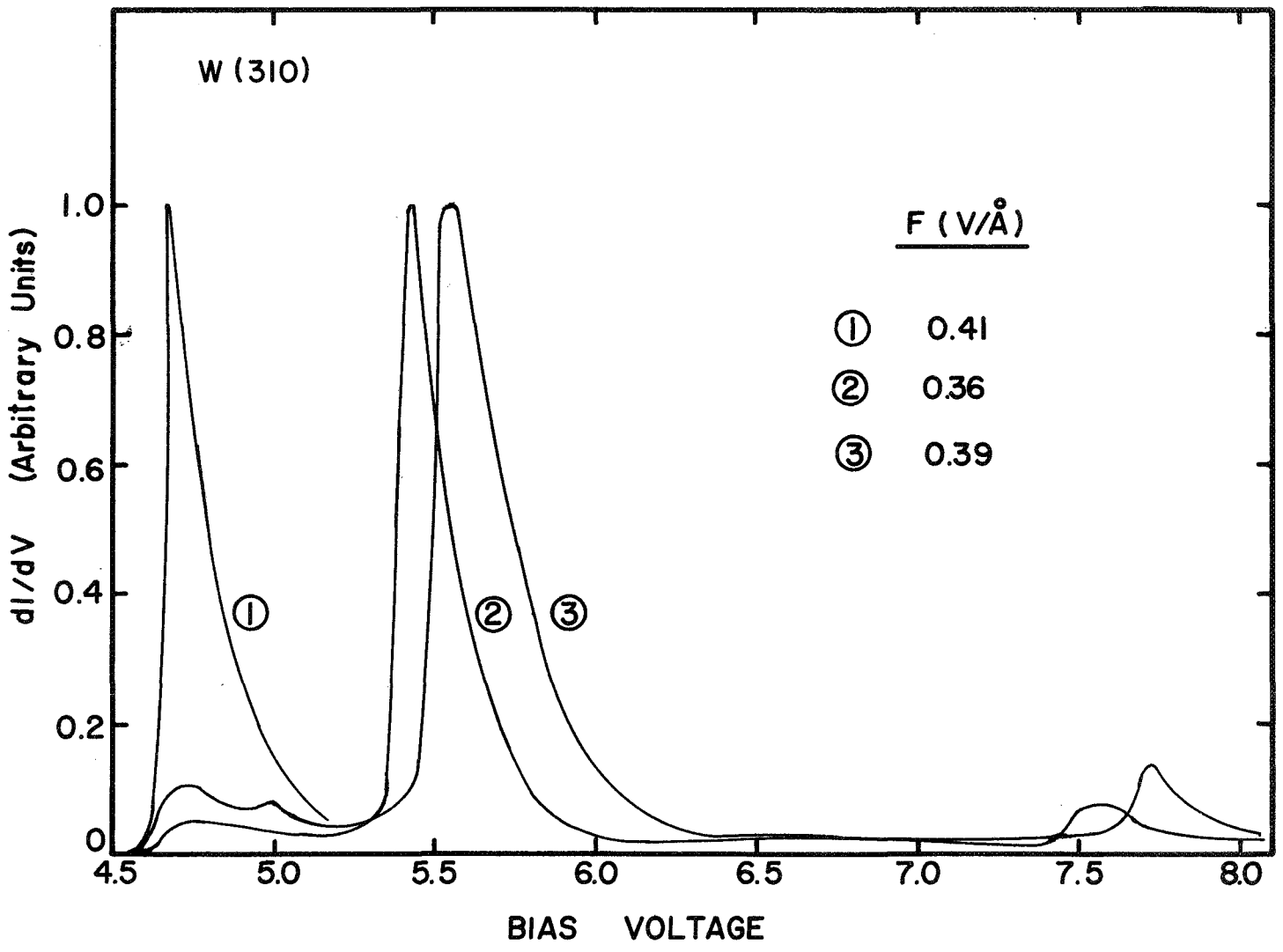

Figure 21 TED spectra pentacene on W (310); curve 1 is clean.

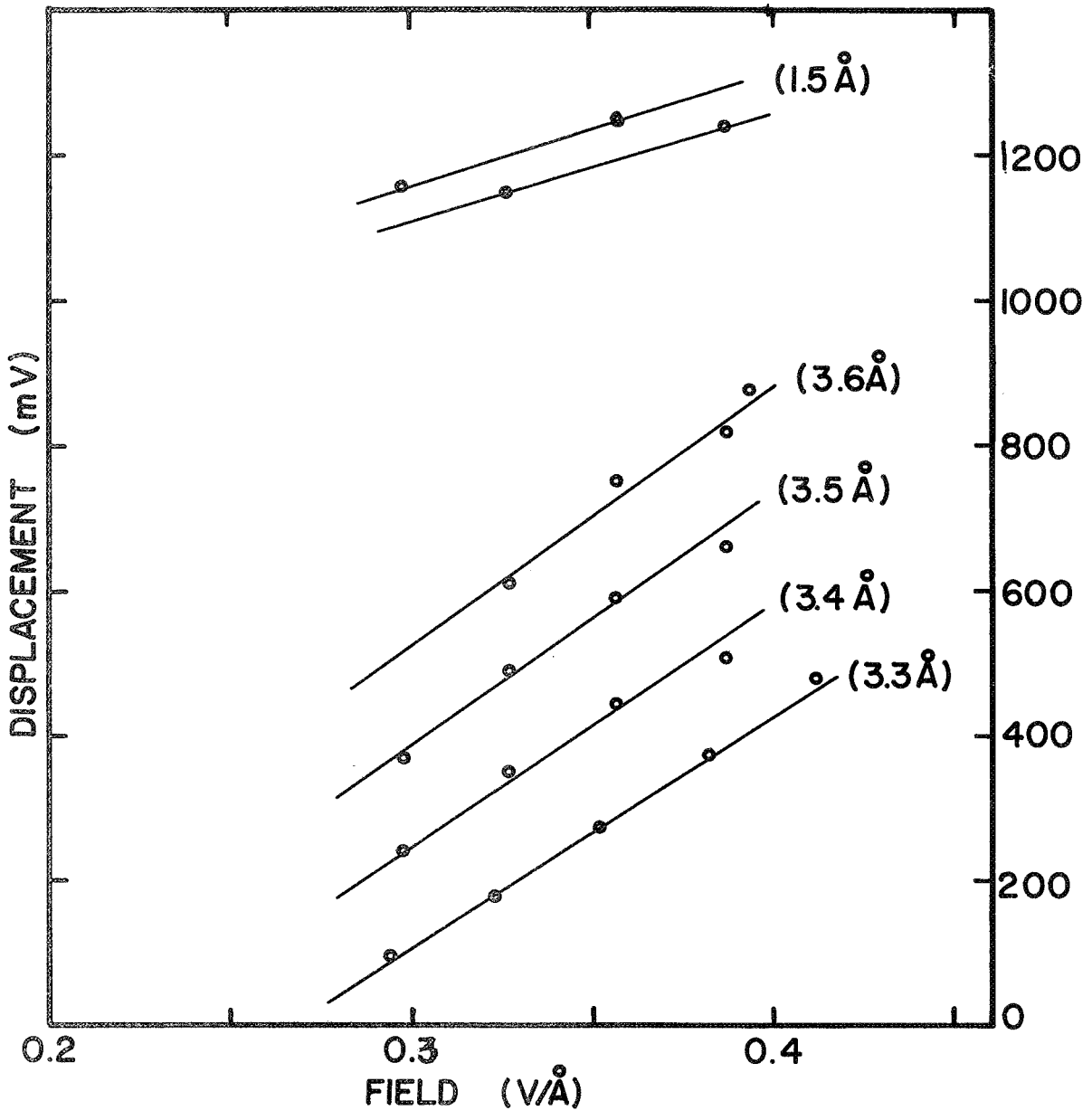

Figure 22 Summary of peak displacements vs field strength for pentacene on W (310).

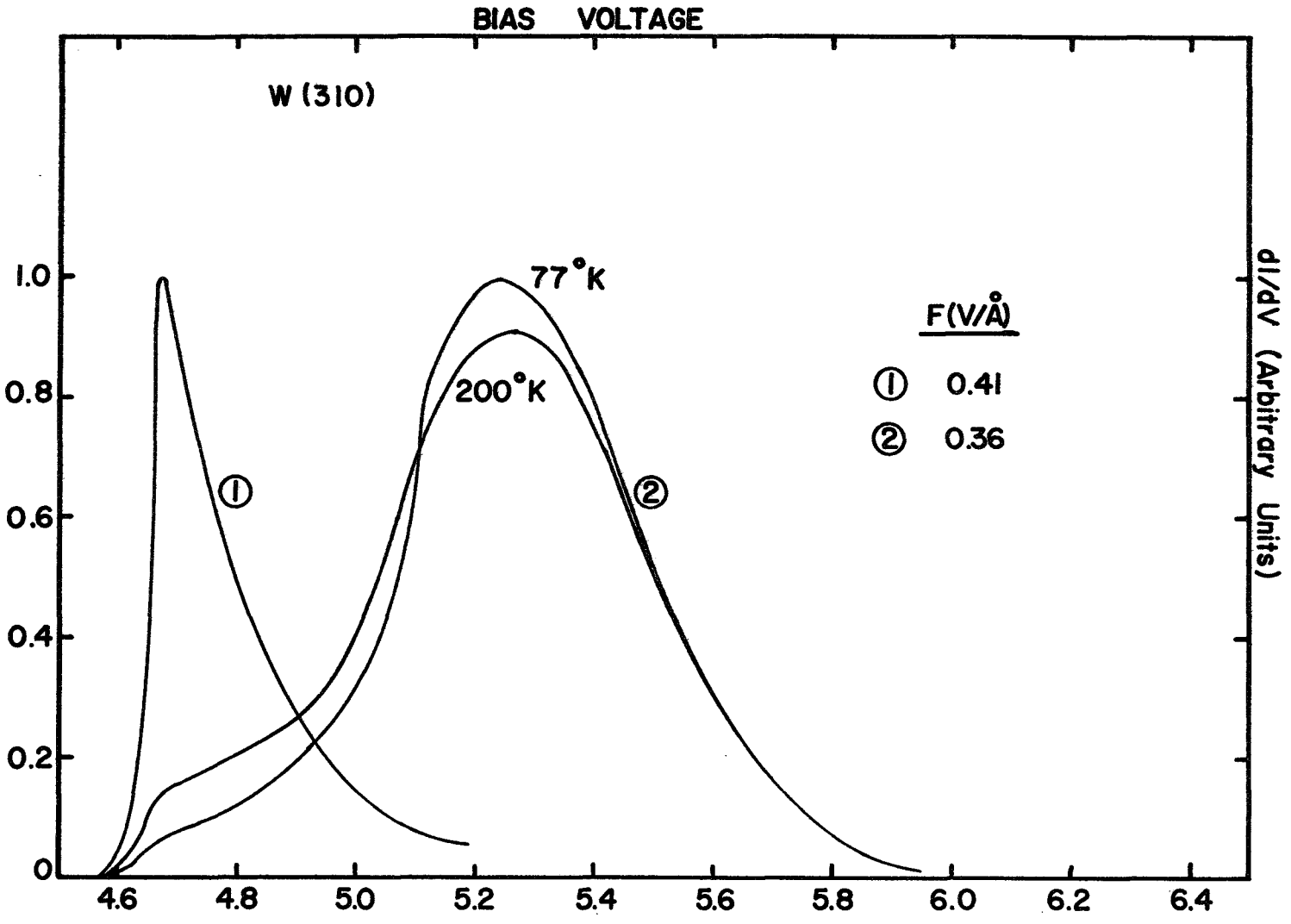

Figure 23 TED spectra pentacene on W (310); curve 1 is clean; $\Delta\phi$ = -0. 65 eV; B = -0. 6; I_a/I_c = 5. 7. The TED is shown at 77 and 200°K.

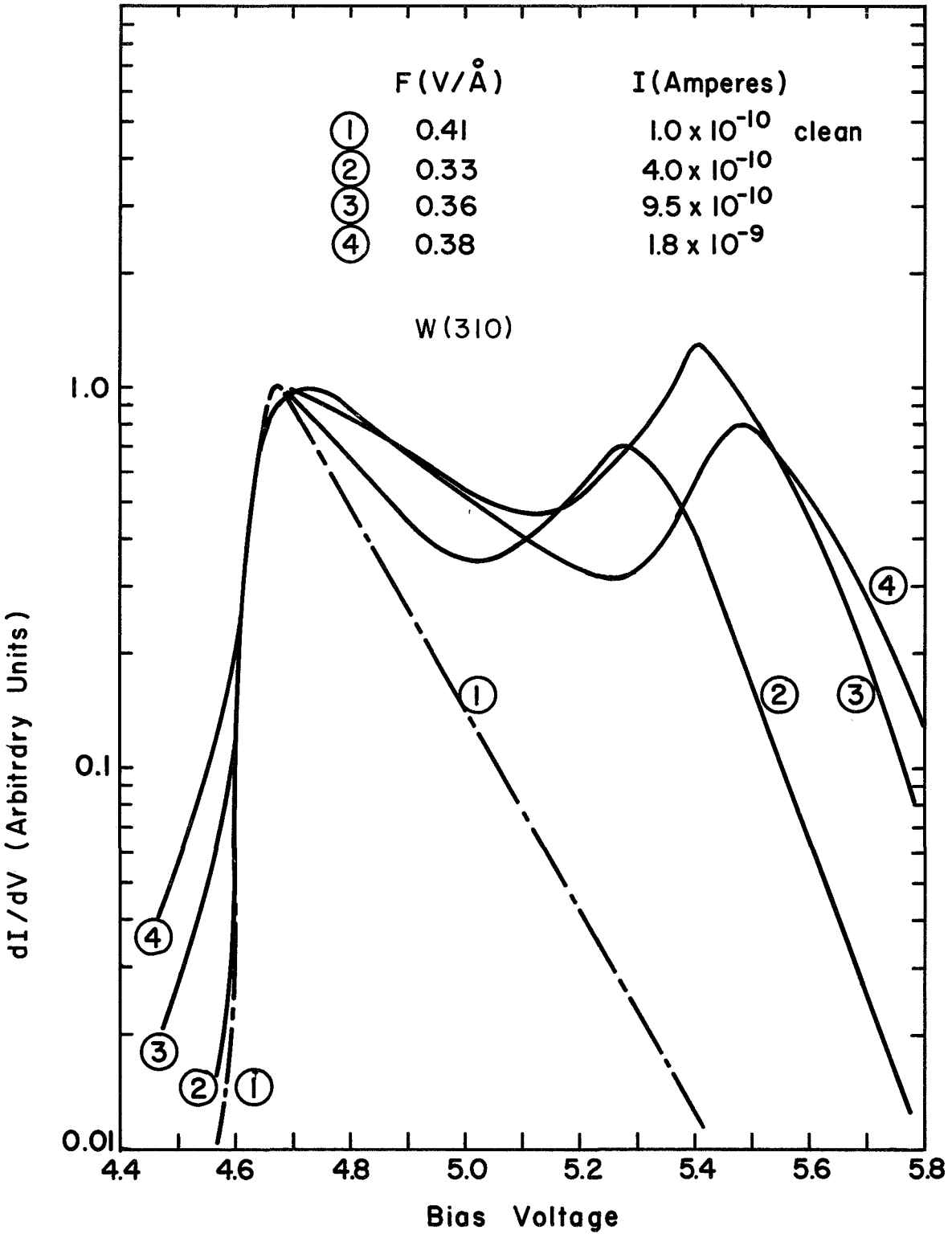

Figure 24 Replot of TED in Figure 20; Note change in leading edge as a function of field (or current).

References

1. J. Lambe and R. Jaklevic, Phys. Rev. 165 821 (1968).
2. W. Thompson, Phys. Rev. Letters 20 , 1085 (1968).
3. C. Duke and M. Alferieff, J. Chem. Phys. 46, 923 (1967).
4. L. Swanson and L. Crouser, Progress Rept. , Contract NASw-1516, Nov. 1968.
5. D. Scalapino and S. Marcus, Phys. Rev. Letters 18, 459 (1967).
6. A. Bennett and L. Falicou 151, 512 (1966).
7. D. Bohm, "Quantum Theory", Prentice Hall Inc. p. 461, 470.
8. E. Plummer, J. Gadzuk and R. Young, Solid State Comm. 7, 487 (1969).
9. A. Ebert and H. Gottlieb J. Am. Chem. Soc. 74, 2806 (1952).
10. G. Herlmeier and G. Warfield, J. Chem. Phys. 38, 893 (1963).
11. A. Sidorou and I. Kotlyar, Optics and Spectroscopy 11, 92 (1961).